

Petrology and retrograde $P-T$ path in granulites of the Kanskaya formation, Yenisey range, Eastern Siberia

LEONID PERCHUK AND TARAS GERYA

Institute of Experimental Mineralogy of the USSR Academy of Sciences

ALEX NOZHIN

Institute of Geology and Geophysics of the Siberian Branch of the USSR Academy of Sciences

ABSTRACT The Kanskaya formation in the Yenisey range, Eastern Siberia is a newly studied example of retrogression of granulite facies rocks. The formation consists of two stratigraphical units: the lower Kuzeevskaya group and the upper Atamanovskaya group. Rocks from both of these units show rare reaction textures such as replacement of cordierite by garnet, sillimanite and quartz, sillimanite coronas around spinel and corundum, and garnet rims around plagioclase in metabasites, while plagioclase rims around garnet can be seen in associated metapelites. The paragenesis quartz + orthopyroxene + sillimanite is a feature of the Kuzeevskaya group. In many samples, chemical zoning of garnet and cordierite shows an increase in Mg from core to rim as well as the reverse.

Biotite–garnet–cordierite–sillimanite–quartz as well as spinel±biotite–garnet±cordierite±sillimanite–quartz assemblages were studied using geothermometers and geobarometers based on both exchange and net-transfer reactions (Perchuk & Lavrent'eva, 1983; Aranovich & Podlesskii, 1983; Gerya & Perchuk, 1989). Detailed investigation of 10 samples including 1000 microprobe analyses revealed decompression (first stage) followed by the near isobaric cooling of the granulites. From geological studies, the 7 km total thickness of the sequence closely corresponds to the pressure difference (~2.2 kbar) measured by geobarometers in the samples taken from different levels in the sequence. Individual samples yield $P-T$ paths ranging from 100° C/kbar to 140° C/kbar depending on their locations with respect to the large Tarakskiy granite pluton. In places the 100° C/kbar path changed to the 140° C/kbar due to the influence of the intrusion. In a $P-T$ diagram these trajectories are subparallel lines, whose $P-T$ maxima define the Archaean geotherm between 3.1 and 2.7 Ga, determined isotopically. A petrological model for $P-T$ evolution of the Kanskaya formation is proposed.

Key words: decompression; granulites; isobaric cooling; retrogression.

List of abbreviations

Ab	= albite	Pl	= plagioclase
Alm	= almandine	Prp	= pyrope
An	= anorthite	Qtz	= quartz
Bt	= biotite	Sil	= sillimanite
Crn	= corundum	Spl	= spinel
Crd	= cordierite	<i>t</i>	= temperature, °C
Cpx	= clinopyroxene	<i>T</i>	= temperature, K
En	= enstatite	<i>P</i>	= pressure, bar
Fe	= ferrosilite	<i>X_i</i>	= mole fraction of component <i>i</i>
Kfs	= K-feldspar	<i>N_i</i>	= mole per cent of component <i>i</i>
Grt	= garnet	<i>W_{ij}</i>	= interaction parameter
Grs	= grossularite	<i>G</i>	= Gibbs free energy, cal
Ilm	= ilmenite	<i>H</i>	= enthalpy, cal
Hbl	= hornblende	<i>S</i>	= entropy, cal
Hc	= hercynite	<i>V</i>	= volume, cal/bar
Mag	= magnetite	Φ^e	= excess thermodynamic function for a solid solution
Ol	= olivine		
Opx	= orthopyroxene		

INTRODUCTION

Studies of granulite facies rocks in different geostructures of the continental crust each year yield new results due to the new methods used. Physico-chemical analyses of mineral parageneses of the rocks and data on fluid inclusions show that the prograde stage of metamorphism is generally not recorded by either mineral reactions or textures, while retrogression is preserved in detail. This rule has been exemplified by evolution of granulite facies rocks from the Hankay central massif, the Aldan shield province and the Sharyzhalgay complex in the southern part of the Siberian platform (Lavrent'eva, 1983; Perchuk, Kitsul, Podlesskii, Gerasimov, Aranovich & Fed'kin, 1981; Perchuk, Aranovich, Podlesskii, Lavrent'eva, Gerasimov, Fed'kin, Kitsul, Karsakov & Berdnikov, 1985; Perchuk, 1989). In many cases a decrease in temperature and pressure is only a characteristic of monocyclic metamorphic complexes (Perchuk, 1983, 1985, 1988) whereas polycyclic metamorphic formations show more than one $P-T$ path.

Of specific interest are those granulite formations whose metamorphic evolution is related to granite magmatism (Korzhinskiy, 1936, 1945; Wells, 1980). The Kanskaya formation of the Angaro-Kanskiy inlier in the Yenisey range, Eastern Siberia provides a good example of such relationships due to the preservation of the Archaean initial stratigraphical sequences metamorphosed in the granulite facies and recorded by $P-T$ changes during Proterozoic retrogression.

GEOLOGICAL OUTLINE

The Yenisey range foldbelt of 700 km length and 150 km width occupies a southern margin of the Siberian platform. Figure 1 shows that the Precambrian granulite facies metasedimentary and metamagmatic rocks form a basement of the foldbelt. The rocks can be subdivided into several complexes. However, this paper is devoted to one of them, namely the Kanskaya formation, which can be further subdivided into two units metamorphosed in the granulite facies: a lower unit referred to as the Kuzeevskaya group and an upper unit known as the Atamanovskaya group. Both units are exposed in the southern part of the Yenisey range (see Fig. 1). In the north-eastern part of the Kanskaya formation the granulite facies rocks of the Atamanovskaya group gradually pass into the granite-gneiss and migmatite zones which further grade into the Tarakskiy granite pluton. All the rocks in this area form a dome geostructure 100 km in length and 15 km in width. Available radiometric age data for rocks of the Kanskaya formation range from 4.1 to 0.8 Ga. The data obtained by the $^{206}\text{Pb}/^{207}\text{Pb}$ method and the Rb/Sr isochron method reflect both the geodynamic and metamorphic history of the region (Gerling & Artemov, 1964; Nozhkin *et al.*, 1989). The Early Proterozoic age (1.8–2.0 Ga) of the Tarakskiy granite pluton is fixed by potassium argon (Artemov, 1963) and the $^{206}\text{Pb}/^{207}\text{Pb}$ method suggested by Volobuev, Zykov & Stupnikova (1980).

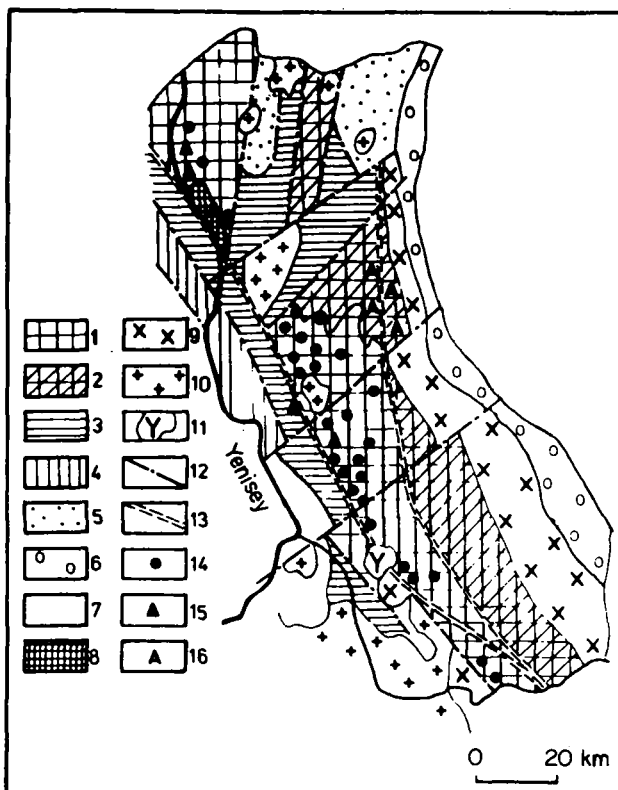


Fig. 1. A schematic geological map of the Angaro-Kanskiy inlier in the Yenisey range. *Precambrian metamorphic rocks:* 1 and 2 – Kuzeevskaya and Atamanovskaya groups, respectively, in the Kanskaya formation; 3 – Yeniseyskaya formation; 4 – Yukseevskaya formation; Late Precambrian volcanics (5) and sediments (6); 7 – Phanerozoic cover. *Magmatic rocks:* 8 – metagabbroids; 9 – Early Precambrian granitoids; 10 – Late Precambrian granitoids; 11 – Middle Palaeozoic volcanics and related plutonic rocks. *Tectonic units:* 12 – faults; 13 – mylonite zones. *Localities of orthopyroxene-sillimanite-quartz assemblages* (14), garnet-clinopyroxene metagabbroids (15) and andalusite bearing rocks (16) after Serenko (1969).

Kuznetsov (1941) and Nozhkin (1983) distinguished the following rock types.

Gneisses – thin-banded and fine-grained quartz-bearing rocks of acid and andesitic bulk composition. The rocks do not contain clinopyroxene and hornblende and can be subdivided into two groups: (i) plagiogneisses ($\text{Qtz} \pm \text{Pl} \pm \text{Opx} \pm \text{Bt} \pm \text{Grt} \pm \text{Kfs}$) and (ii) metapelites ($\text{Qtz} + \text{Pl} + \text{Kfs} \pm \text{Grt} \pm \text{Crd} \pm \text{Opx} \pm \text{Bt} \pm \text{Sil} \pm \text{Crn} \pm \text{Spl} \pm \text{And}$).

Charnockites and enderbites of magmatic and metamorphic origin can be recognized in terms of texture and relationships with wall rocks. Magmatic charnockites and enderbites show a typical massive texture and quite a constant bulk composition. The rocks form cross-cutting and concordant bodies among gneisses while metamorphic charnockites and enderbites are coarse-grained biotite-garnet-hypersthene rocks interlayered with gneisses.

Metabasites are represented by fine-grained metabasalts ($\text{Cpx} + \text{Pl} \pm \text{Grt} \pm \text{Hb} \pm \text{Bt} \pm \text{Qtz}$) and metagabbroids. Metamorphosed under granulite facies $P-T$ conditions,

the latter rocks (originally gabbro, gabbro-norite, norite, anorthosite, diorite and pyroxenite) form bands, lenses and boudins up to 300 m thick and 2 km long as well as layered massifs which are up to 25 km in diameter and 1.5 km thick.

Plagiogneisses, two-feldspar gneisses and charnockites with a relatively small quantity of metapelites, gneisses and metagabbroids are characteristic of the Kuzeevskaya group. The Atamanovskaya group is mainly composed of two-feldspar gneisses and metapelites with a small amount of plagiogneisses. Metabasites are practically absent from the Atamanovskaya group. An average composition of the Kanskaya formation corresponds to granodiorite.

The AFM diagram in Fig. 2 illustrates the petrochemical features of the Kanskaya formation: the metabasites of the Kuzeevskaya group reflect Fe/Mg differentiated series while granites, gneisses and charnockites show a trend unrelated to the basaltic magmatism. Perchuk (1989) describes similar relationships for the Sharyzhalgay

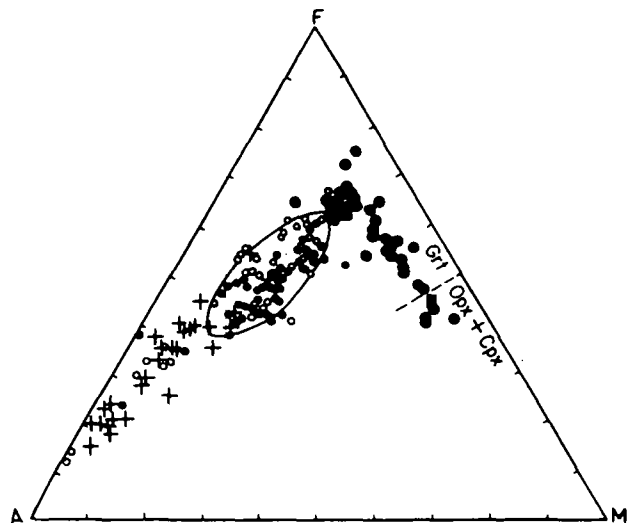


Fig. 2. The AFM diagram for the rocks of the Kanskaya formation. ● = biotite-garnet-hypersthene gneisses, ●• = basic granulites with garnet (grt) and/or pyroxenes (Cpx + Opx), ○ = charnockites and enderbites, ■ = metagabbroid, + = granites of the Tarakskiy pluton.

Table 1. Mineral assemblages of metapelites from the the Kanskaya Formation in the Yenisey range. Symbols: (+) = mineral present, (*) = mineral has been analysed and chemical zoning has been recognized in it, (-) = mineral not present. Both quartz and corundum were present in the sample, but sillimanite rims are always formed at the contacts of the minerals.

Sample	Qtz	Pl	Kfs	Grt	Bt	Opx	Crd	Spl	Sil	Crn	Ilm	Mag	Gr
Atamanovskaya group													
A-257	+	+	+	*	*	-	*	+	+	-	-	+	-
A-258	+	+	+	*	*	-	*	*	+	-	-	+	-
A-269	+	*	*	*	*	-	*	-	-	-	-	+	-
A-275	+	+	+	*	*	-	*	+	+	-	-	+	-
A-538	+	*	*	*	*	+	*	*	+	-	+	-	+
A-643	+	*	*	*	*	-	*	*	+	+	+	+	-
Kuzeevskaya group													
K-106	+	+	+	*	*	-	*	+	+	-	+	+	+
K-111	+	*	*	*	*	-	*	*	+	-	+	-	+
K-115	+	*	*	*	*	+	*	+	+	-	+	+	-
K-119	+	+	*	*	*	-	*	+	+	+	+	+	-
K-170	+	*	*	*	*	-	*	+	+	+	+	-	+
K-302	+	+	+	*	*	-	*	*	+	-	+	-	+

metamorphic complex exposed along the south-eastern Baikal shore.

An initial tholeiitic composition for the metabasites is supported by geological, geochemical and rock texture observations; all metabasites of the Kanskaya formation and Sharyzhalgay complex were formed from tholeiitic basalts. Charnockites and gneisses form a separate series which is petrochemically independent of metabasites (Fig. 2).

Near the Tarakskiy pluton, metapelites of the Atamanovskaya group may contain andalusite while orthopyroxene-sillimanite-quartz and clinopyroxene-garnet assemblages are common characteristics of the Kuzeevskaya group (see Fig. 1). Metamorphic grade increases from the Tarakskiy pluton toward the Yenisey-skii complex.

MINERAL CHEMISTRY

The mineral chemistry of the Kanskaya formation rocks is based on several hundred microprobe analyses. The mineral assemblages of major varieties of the Kanskaya formation metamorphic rocks are given in Table 1. In this section we consider only those minerals which provide information on the conditions of metamorphic evolution of the Kanskaya granulite facies formation. Some representative mineral analyses are shown in Tables 2-4.

Garnet. The compositions of garnet and its textural relationships with other minerals reflect different stages in the metamorphic evolution of the Kanskaya formation. The garnet composition varies within a relatively wide range depending on the bulk rock chemistry as well as physical conditions of local equilibria. In metabasites garnet appears at the weight ratio of the rocks of $Fe/Mg > 1$ (Fig. 2). Figure 3 demonstrates the main features of garnet chemistry. All garnets in the Kanskaya formation rocks show chemical zoning. Histograms in Fig. 4 illustrate the changes of contents of some elements between the rims and cores of the garnet grains. In many granulites from the Kanskaya formation N_{Mg}^{Grt} increases toward the rims of the garnet grains! In such cases, compositions of rims of large grains correspond to small newly formed crystals of garnet in cordierite (see Fig. 9a) or plagioclase matrices.

Representative analyses of garnets used for geothermometry and geobarometry are listed in Table 2.

Biotites are characterized by a common negative correlation between Al and Mg contents. Mg/Fe ratios for biotites from the rocks of the Kuzeevskaya group are essentially higher than those of the Atamanovskaya group. Other features of biotite chemistry

Table 2. Microprobe analysis and cation ratios in garnets from metapelites of the Atamanovskaya (A) and Kuzeevskaya (K) groups of the Kanskaya metamorphic formation.

Sample Spot no.	A-257 42	A-257 48	A-257 59	A-257 61	A-258 1	A-258 10	A-258 69	A-258 E2	A-258 E6	A-258 66	A-258 E8	A-269 73	A-269 75	A-269 77	A-275 41	A-275 D30
SiO ₂	37.30	37.01	37.46	37.31	37.40	37.17	37.21	36.96	36.76	38.13	36.94	36.52	36.45	36.18	37.15	36.39
Al ₂ O ₃	20.72	21.00	20.58	20.72	20.81	20.95	20.35	20.46	20.81	20.81	20.42	20.37	20.35	20.07	20.88	21.22
FeO	34.98	35.69	35.72	35.28	33.54	33.65	35.62	34.88	34.13	33.36	34.58	36.16	37.22	36.67	35.82	36.32
MnO	1.08	0.69	0.76	0.08	2.69	2.71	1.40	2.84	2.66	0.77	2.40	0.32	0.21	0.04	0.30	0.56
MgO	4.84	4.67	4.56	4.71	4.53	4.40	4.65	4.22	4.88	6.43	5.17	4.80	4.42	3.99	4.59	4.56
CaO	1.01	0.62	0.54	1.00	1.03	1.11	0.39	0.61	0.75	0.40	0.48	1.15	1.06	2.98	1.10	0.91
Total	99.93	99.68	99.62	99.82	100.00	99.99	99.62	99.97	99.99	99.90	99.99	99.32	99.71	99.93	99.84	99.96
Cations based on 12 oxygens																
Si	2.990	2.977	3.013	2.994	2.996	2.982	3.002	2.984	2.957	3.018	2.972	2.962	2.957	2.940	2.983	2.932
Al	1.958	1.991	1.951	1.960	1.956	1.981	1.935	1.947	1.973	1.941	1.936	1.947	1.946	1.922	1.976	2.015
Fe	2.345	2.401	2.403	2.368	2.247	2.258	2.404	2.355	2.296	2.208	2.327	2.453	2.525	2.492	2.405	2.448
Mn	0.073	0.047	0.052	0.054	0.183	0.184	0.096	0.194	0.181	0.052	0.164	0.022	0.014	0.003	0.020	0.038
Mg	0.578	0.560	0.547	0.564	0.541	0.526	0.559	0.508	0.585	0.759	0.620	0.580	0.535	0.483	0.549	0.548
Ca	0.087	0.053	0.046	0.086	0.088	0.095	0.034	0.053	0.065	0.034	0.041	0.100	0.092	0.260	0.095	0.079
Total	8.031	8.028	8.012	8.026	8.021	8.027	8.030	8.041	8.057	8.012	8.060	8.064	8.070	8.099	8.029	8.060
X _{Mg} ^{Grt}	0.193	0.186	0.182	0.189	0.182	0.177	0.183	0.166	0.191	0.251	0.199	0.190	0.174	0.162	0.185	0.180

Table 2. (Continued.)

Sample Spot no.	A-275 117	A-275 40	A-538 100	A-538 103	A-538 105	A-538 124	A-538 126	A-538 130	A-538 104	A-538 107	A-538 140	A-538 202	A-538 148	A-538 153	A-538 37	A-643 P52
SiO ₂	37.04	37.40	38.05	38.29	38.01	37.71	37.92	37.62	37.92	37.91	37.76	37.56	37.93	37.99	37.98	37.36
Al ₂ O ₃	20.81	21.03	21.34	21.01	21.18	21.66	21.04	21.00	21.28	21.38	21.16	21.19	21.35	21.33	20.95	20.57
FeO	35.95	35.49	32.72	33.65	32.95	32.22	33.86	33.09	33.41	33.84	34.13	32.06	33.23	34.13	34.74	
MnO	0.37	0.48	0.17	0.00	0.00	0.14	0.00	0.18	0.00	0.00	0.00	0.00	0.11	0.00	0.12	0.42
MgO	4.52	4.29	6.81	5.99	6.56	6.31	6.28	6.82	6.37	6.08	5.73	5.65	7.02	6.55	6.05	6.05
CaO	1.26	1.20	0.85	1.05	1.20	0.70	0.86	0.81	0.96	0.70	1.13	0.96	0.97	0.62	0.70	0.85
Total	99.95	99.89	99.94	99.99	99.90	99.74	99.96	99.53	99.94	99.91	99.62	99.49	99.44	99.72	99.93	99.99
Cations based on 12 oxygens																
Si	2.976	2.997	2.996	3.024	2.999	2.982	3.001	2.985	2.995	2.998	3.001	2.993	2.994	3.001	3.010	2.980
Al	1.971	1.986	1.981	1.956	1.970	2.019	1.962	1.964	1.981	1.993	1.982	1.990	1.986	1.986	1.957	1.934
Fe	2.416	2.378	2.155	2.223	2.174	2.197	2.241	2.196	2.207	2.238	2.249	2.275	2.116	2.195	2.262	2.318
Mn	0.025	0.033	0.011	0.000	0.000	0.009	0.000	0.012	0.000	0.000	0.000	0.007	0.000	0.008	0.028	
Mg	0.541	0.512	0.799	0.075	0.772	0.744	0.741	0.807	0.750	0.717	0.679	0.671	0.826	0.771	0.715	0.719
Ca	0.108	0.103	0.072	0.089	0.102	0.059	0.073	0.070	0.081	0.059	0.096	0.082	0.082	0.052	0.059	0.073
Total	8.038	8.010	8.014	7.997	8.017	8.010	8.018	8.034	8.014	8.005	8.008	8.011	8.011	8.005	8.011	8.053
X _{Mg} ^{Grt}	0.181	0.175	0.270	0.241	0.262	0.252	0.248	0.268	0.254	0.243	0.232	0.228	0.280	0.260	0.239	0.235

Table 2. (Continued.)

Sample Spot no.	A-643 P10	A-643 P31	A-643 P37	A-643 P17	A-643 P25	A-643 P26	A-643 P64	A-643 P65	K-106 11	K-106 2	K-106 5	K-106 9	K-111 49	K-111 61	K-111 68	K-111 CS
SiO ₂	36.98	37.38	37.47	36.88	36.50	36.90	36.33	36.36	38.02	37.44	38.13	37.76	38.12	38.20	38.49	39.08
Al ₂ O ₃	20.46	20.51	20.44	20.64	20.29	20.51	20.53	20.43	21.03	21.01	21.16	20.98	20.90	21.73	21.12	21.08
FeO	35.70	34.81	34.54	35.54	36.07	35.60	36.85	37.35	32.58	33.53	33.08	33.30	32.95	29.85	30.92	30.45
MnO	0.39	0.52	0.52	0.39	0.39	0.27	0.22	0.18	0.12	0.20	0.17	0.02	0.00	0.00	0.00	0.00
MgO	5.35	5.60	5.71	5.43	5.40	5.37	4.93	4.47	6.87	6.36	6.55	6.42	6.83	9.02	8.15	8.08
CaO	1.03	1.04	1.12	0.89	1.07	1.24	1.05	1.12	1.27	1.17	0.88	1.02	1.08	1.14	1.06	1.25
Total	99.91	99.86	99.80	99.77	99.72	99.89	99.91	99.89	99.71	99.97	99.50	99.88	99.94	99.74	99.94	
Cations based on 12 oxygens																
Si	2.970	2.990	2.995	2.963	2.948	2.964	2.937	2.946	2.998	2.976	3.006	2.998	3.008	2.968	3.010	3.040
Al	1.937	1.933	1.926	1.955	1.932	1.942	1.956	1.951	1.955	1.968	1.967	1.963	1.944	1.990	1.947	1.933
Fe	2.398	2.328	2.309	2.388	2.437	2.391	2.491	2.531	2.149	2.229	2.181	2.211	2.174	1.940	2.022	1.981
Mn	0.026	0.035	0.025	0.026	0.027	0.018	0.015	0.012	0.008	0.013	0.011	0.001	0.000	0.000	0.000	0.000
Mg	0.641	0.668	0.680	0.650	0.650	0.643	0.594	0.540	0.808	0.754	0.770	0.760	0.803	1.045	0.950	0.936
Ca	0.089	0.089	0.096	0.077	0.093	0.107	0.091	0.097	0.107	0.100	0.074	0.087	0.091	0.095	0.089	0.104
Total	8.061	8.043	8.042	8.059	8.087	8.065	8.084	8.077	8.024	8.040	8.010	8.020	8.020	8.037	8.017	7.994
X _{Mg} ^{Grt}	0.209	0.220	0.225	0.212	0.209	0.211	0.192	0.175	0.272	0.252	0.260	0.256	0.270	0.350	0.320	0.321

Table 2. (Continued.)

Sample Spot no.	K-111 42	K-111 53	K-111 56	K-115 24	K-115 47	K-115 49	K-115 62	K-119 33	K-119 37	K-119 40	K-170 109	K-170 112	K-170 114	K-170 91	K-170 93	K-302 17
SiO ₂	38.33	37.86	37.78	38.65	38.58	39.04	38.22	38.82	38.89	38.03	37.78	37.70	37.83	38.21	37.70	30.20
Al ₂ O ₃	20.58	21.10	21.40	21.32	21.13	21.35	21.21	21.53	21.51	21.49	21.12	21.24	21.01	21.16	21.23	21.30
FeO	32.43	32.00	31.63	29.66	30.54	29.62	31.15	29.15	29.43	29.76	30.84	31.10	31.93	29.63	30.62	28.60
MnO	0.00	0.00	0.00	0.36	0.11	0.22	0.30	0.07	0.19	0.00	0.09	0.06	0.00	0.22	0.00	0.17
MgO	6.92	7.59	7.66	9.46	9.05	9.34	8.78	9.14	8.66	8.76	8.63	8.51	8.01	9.58	9.30	8.15
CaO	1.17	1.20	1.17	0.32	0.37	0.43	0.34	1.15	1.22	1.42	0.99	1.17	1.09	1.13	1.02	1.02
Total	99.43	99.75	99.64	99.77	99.78	100.00	100.00	99.86	99.90	99.46	99.45	99.78	99.87	99.93	99.87	98.44
Cations based on 12 oxygens																
Si	3.031	2.981	2.972	3.001	3.005	3.019	2.984	3.005	3.015	2.973	2.969	2.958	2.974	2.972	2.947	3.067
Al	1.918	1.958	1.985	1.951	1.940	1.946	1.952	1.965	1.965	1.980	1.956	1.964	1.947	1.940	1.956	1.964
Fe	2.145	2.107	2.081	1.926	1.990	1.916	2.034	1.887	1.908	1.945	2.027	2.041	2.100	1.927	2.002	1.871
Mn	0.000	0.000	0.000	0.024	0.007	0.014	0.020	0.005	0.013	0.000	0.006	0.004	0.000	0.015	0.000	0.011
Mg	0.816	0.891	0.898	1.095	1.051	1.077	1.022	1.055	1.001	1.021	1.011	0.995	0.939	1.111	1.084	0.951
Ca	0.099	0.101	0.099	0.027	0.031	0.036	0.028	0.095	0.101	0.119	0.083	0.098	0.092	0.094	0.085	0.086
Total	8.009	8.038	8.035	8.023	8.024	8.008	8.040	8.012	8.003	8.037	8.053	8.060	8.052	8.058	8.075	7.950
X _{Mg} ^{Grt}	0.276	0.297	0.301	0.360	0.345	0.358	0.332	0.358	0.343	0.344	0.332	0.327	0.309	0.364	0.351	0.336

Table 2. (Continued.)

Sample Spot no.	K-302 R32	K-302 R33	K-302 R43	K-302 24	K-302 26	K-302 30
SiO ₂	38.54	38.00	38.37	38.42	38.45	37.86
Al ₂ O ₃	21.80	22.01	21.85	21.07	21.04	21.06
FeO	29.95	30.98	30.33	30.89	31.19	32.71
MnO	0.01	0.00	0.00	0.00	0.08	0.07
MgO	8.14	7.69	7.93	8.18	7.86	6.82
CaO	1.15	0.87	1.22	1.15	1.13	1.06
Total	99.59	99.55	99.70	99.71	99.75	99.58
Cations based on 12 oxygens						
Si	3.002	2.976	2.992	3.006	3.012	2.995
Al	2.001	2.031	2.009	1.943	1.943	1.964
Fe	1.951	2.029	1.978	2.022	2.043	2.164
Mn	0.001	0.000	0.000	0.000	0.005	0.005
Mg	0.945	0.898	0.922	0.954	0.918	0.804
Ca	0.096	0.073	0.102	0.096	0.095	0.090
Total	7.996	8.007	8.003	8.022	8.017	8.023
X _{Mg} ^{Grt}	0.326	0.307	0.318	0.321	0.309	0.271

Table 3. Microprobe analysis and cation ratios in biotites from metapelites of the Atamanovskaya (A) and Kuzeevskaya (K) groups of the Kanskaya metamorphic formation.

Sample Spot no.	A-257 57	A-257 60	A-258 68	A-258 70	A-269 72	A-269 76	A-275 39	A-275 53	A-538 135	A-538 139	A-643 P30	A-643 P46	K-106 1	K-106 16	K-111 60	K-111 67
SiO ₂	38.10	37.19	38.20	36.82	36.74	36.82	39.99	36.84	37.50	38.25	38.15	37.50	39.12	39.12	38.28	39.8
TiO ₂	1.35	4.96	4.80	5.07	4.84	5.08	2.77	5.43	6.51	5.87	5.22	5.22	4.36	5.05	5.97	5.15
Al ₂ O ₃	18.49	16.35	15.99	16.22	16.18	16.46	15.71	16.33	15.68	16.42	15.20	15.31	16.19	15.68	15.13	15.88
FeO	16.83	19.16	16.27	20.69	19.52	19.21	15.94	21.17	15.64	14.21	15.80	18.76	12.38	13.67	14.18	10.63
MgO	14.60	11.47	13.48	10.14	11.60	11.17	15.05	9.48	13.02	14.18	14.25	12.26	16.82	15.31	14.53	17.56
Na ₂ O	0.48	0.13	0.00	0.00	0.18	0.24	0.58	0.19	0.00	0.19	0.00	0.00	0.32	0.17	0.00	0.00
K ₂ O	10.14	10.74	11.04	10.92	10.94	11.03	10.96	10.57	11.37	10.51	11.20	10.88	10.80	11.00	10.96	10.46
Total	99.99	100.00	99.78	99.86	100.00	100.01	101.00	100.01	99.72	99.63	99.82	99.93	99.99	100.00	99.05	99.53
Cations based on 11 oxygens																
Si	2.727	2.712	2.753	2.712	2.692	2.693	2.834	2.711	2.709	2.727	2.749	2.735	2.758	2.776	2.756	2.787
Ti	0.073	0.272	0.260	0.281	0.267	0.280	0.148	0.300	0.354	0.315	0.283	0.286	0.231	0.270	0.323	0.271
Al	1.560	1.405	1.358	1.408	1.397	1.419	1.312	1.416	1.335	1.380	1.291	1.316	1.345	1.312	1.284	1.309
Fe	1.007	1.169	0.981	1.275	1.196	1.175	0.945	1.303	0.945	0.847	0.952	1.144	0.730	0.811	0.854	0.622
Mg	1.558	1.247	1.448	1.113	1.267	1.218	1.590	1.040	1.402	1.507	1.531	1.333	1.767	1.620	1.559	1.831
Na	0.067	0.018	0.000	0.000	0.026	0.034	0.080	0.027	0.000	0.026	0.000	0.000	0.044	0.023	0.000	0.000
K	0.926	0.999	1.015	1.026	1.023	1.029	0.991	0.992	1.048	0.956	1.030	1.012	0.971	0.996	1.007	0.933
Total	7.917	7.822	7.815	7.816	7.867	7.849	7.898	7.790	7.793	7.759	7.837	7.827	7.846	7.808	7.782	7.754
X _{Mg} ^{Bt}	0.607	0.516	0.596	0.466	0.514	0.509	0.627	0.444	0.597	0.640	0.617	0.538	0.708	0.666	0.646	0.747

Table 3. (Continued.)

Sample Spot no.	K-115 49	K-115 51	K-119 35	K-119 39	K-170 111	K-170 113	K-302 23	K-302 27
SiO ₂	39.85	39.51	38.81	40.04	37.60	40.97	38.65	39.45
TiO ₂	4.28	5.13	6.25	4.73	4.61	4.14	6.44	5.84
Al ₂ O ₃	15.79	15.13	14.37	14.95	15.09	14.98	15.87	15.06
FeO	11.06	11.12	13.69	9.83	20.28	9.65	13.56	12.47
MgO	17.67	18.04	15.50	18.79	11.76	18.72	14.19	16.14
Na ₂ O	0.34	0.00	0.40	0.36	0.38	0.00	0.40	0.10
K ₂ O	10.99	11.08	10.97	11.29	10.28	11.53	10.90	10.94
Total	99.98	100.0	99.99	99.99	100.00	99.99	100.01	100.00
Cations based on 11 oxygens								
Si	2.792	2.773	2.765	2.798	2.753	2.853	2.745	2.784
Ti	0.226	0.271	0.335	0.249	0.254	0.217	0.344	0.310
Al	1.304	1.252	1.207	1.231	1.302	1.229	1.329	1.253
Fe	0.648	0.653	0.816	0.575	1.242	0.562	0.805	0.736
Mg	1.846	1.887	1.647	1.957	1.284	1.943	1.502	1.698
Na	0.046	0.000	0.055	0.049	0.054	0.000	0.055	0.014
K	0.983	0.992	0.997	1.007	0.960	1.024	0.988	0.985
Total	7.844	7.827	7.822	7.865	7.849	7.828	7.768	7.779
X _{Mg} ^{Br}	0.740	0.743	0.669	0.773	0.508	0.776	0.651	0.698

Table 4. Microprobe analysis and cation ratios in cordierites from metapelites of the Atamanovskaya (A) and Kuzeevskaya (K) groups of the Kanskaya metamorphic formation.

Sample Spot no.	A-257 47	A-257 49	A-258 85	A-258 E3	A-258 E7	A-258 65	A-258 E13	A-258 E14	A-258 E9	A-269 70	A-275 D25	A-275 D28	A-538 127	A-538 128	A-538 13	A-538 149
SiO ₂	50.36	49.93	49.50	50.64	50.23	50.97	50.35	50.54	50.46	49.34	49.98	51.31	50.11	50.33	50.44	50.49
Al ₂ O ₃	33.46	33.38	32.82	33.02	33.03	32.99	32.85	33.08	33.20	32.66	32.65	32.73	33.71	33.04	32.85	33.08
FeO	6.24	7.26	8.67	6.51	7.27	6.41	6.47	6.18	6.69	8.58	8.74	6.27	4.88	5.04	7.85	5.24
MgO	9.89	9.02	8.74	9.54	9.43	9.35	9.57	10.14	9.46	8.82	8.55	9.20	11.05	11.33	8.69	10.98
Total	99.95	99.59	99.73	99.71	99.96	99.72	99.24	99.94	99.94	99.40	99.92	99.51	99.95	99.74	99.83	99.79
Cations based on 18 oxygens																
Si	5.040	5.038	5.025	5.083	5.051	5.109	5.079	5.058	5.062	5.025	5.061	5.147	4.996	5.028	5.087	5.043
Al	3.947	3.970	3.927	3.907	3.915	3.898	3.905	3.902	3.926	3.921	3.897	3.870	3.961	3.891	3.905	3.894
Fe	0.522	0.613	0.736	0.546	0.611	0.537	0.546	0.517	0.561	0.731	0.740	0.526	0.407	0.421	0.662	0.438
Mg	1.476	1.357	1.323	1.427	1.414	1.397	1.439	1.513	1.415	1.339	1.291	1.376	1.642	1.687	1.306	1.635
Total	10.986	10.977	11.011	10.964	10.991	10.941	10.969	10.990	10.975	11.015	10.990	10.918	11.023	11.027	10.960	11.010
X _{Mg} ^{Crd}	0.739	0.689	0.642	0.723	0.698	0.722	0.725	0.745	0.712	0.647	0.635	0.723	0.795	0.800	0.664	0.789

* All analyses were normalized to 100% involving Na, K, Co, Cr, Zn etc., whose contents are not included in this table.

Table 4. (Continued.)

Sample Spot no.	A-538 151	A-538 152	A-538 155	A-538 162	A-538 164	A-538 18	A-538 2	A-538 22	A-538 165	A-538 26	A-538 25	A-643 P44	A-643 P53	K-106 4	K-106 60	K-111 50
SiO ₂	50.35	49.96	50.49	49.85	50.42	50.51	50.74	50.39	50.17	50.71	50.26	49.94	50.67	51.09	50.47	51.49
Al ₂ O ₃	33.17	33.63	33.36	33.44	33.40	32.93	33.26	32.82	33.38	32.67	32.62	32.78	32.73	33.19	33.03	33.40
FeO	6.15	5.47	5.07	5.52	5.80	7.74	5.92	7.94	5.34	7.78	8.40	7.61	5.76	4.48	6.54	4.13
MgO	10.26	10.60	11.00	10.59	10.33	8.63	10.00	8.61	10.88	8.52	8.50	19.52	10.40	10.86	19.81	10.82
Total	99.93	99.66	99.92	99.52	99.95	99.81	99.92	99.76	99.77	99.68	99.78	99.85	99.56	99.62	99.85	99.84
Cations based on 18 oxygens																
Si	5.041	5.003	5.032	5.004	5.038	5.091	5.070	5.088	5.016	5.117	5.086	5.039	5.080	5.087	5.063	5.103
Al	3.914	3.969	3.919	3.956	3.934	3.912	3.917	3.906	3.934	3.886	3.891	3.899	3.868	3.895	3.906	3.902
Fe	0.515	0.458	0.423	0.463	0.485	0.652	0.495	0.670	0.447	0.656	0.711	0.642	0.483	0.373	0.549	0.342
Mg	1.531	1.582	1.634	1.585	1.539	1.297	1.490	1.296	1.621	1.282	1.282	1.432	1.554	1.612	1.467	1.599
Total	11.001	11.012	11.008	11.018	10.996	10.952	10.972	10.960	11.017	10.940	10.970	11.012	10.986	10.966	10.984	10.946
X _{Mg} ^{Crd}	0.748	0.775	0.794	0.770	0.760	0.665	0.751	0.659	0.784	0.661	0.643	0.690	0.763	0.812	0.728	0.824

Table 4. (Continued.)

Sample Spot no.	K-111 Cl2	K-111 50	K-115 27	K-115 64	K-119 34	K-119 36	K-170 92	K-170 94	K-302 29	K-302 31	K-302 R36	K-302 R37	K-302 R39	K-302 R40
SiO ₂	49.10	51.49	50.46	50.82	51.09	51.13	51.06	51.22	50.82	50.70	50.21	50.16	49.60	49.95
Al ₂ O ₃	32.41	33.40	33.40	33.25	33.49	33.28	33.42	33.44	33.32	32.86	34.35	34.34	34.26	33.96
FeO	6.59	4.13	4.78	3.87	4.04	4.19	4.08	4.73	4.58	6.28	4.08	4.71	5.26	5.68
MgO	19.28	10.82	11.12	11.93	11.07	11.20	11.40	10.51	10.74	9.82	11.11	10.63	10.81	10.31
Total	97.38	99.84	99.76	99.87	99.69	99.80	99.96	99.90	99.46	99.66	99.79	99.96	99.97	99.90
Cations based on 18 oxygens														
Si	5.055	5.103	5.031	5.041	5.073	5.076	5.061	5.088	5.071	5.087	4.989	4.990	4.951	4.993
Al	3.933	3.902	3.925	3.888	3.920	3.895	3.904	3.916	3.919	3.886	4.023	4.027	4.031	4.001
Fe	0.568	0.342	0.399	0.321	0.336	0.348	0.338	0.393	0.382	0.527	0.339	0.392	0.439	0.475
Mg	1.423	1.599	1.653	1.764	1.639	1.658	1.684	1.556	1.597	1.469	1.646	1.577	1.609	1.536
Total	10.979	10.946	11.007	11.015	10.967	10.976	10.987	10.954	10.970	10.970	11.000	10.996	11.033	11.005
$X_{\text{Mg}}^{\text{Crd}}$	0.715	0.824	0.806	0.846	0.830	0.827	0.833	0.798	0.807	0.736	0.828	0.797	0.784	0.764

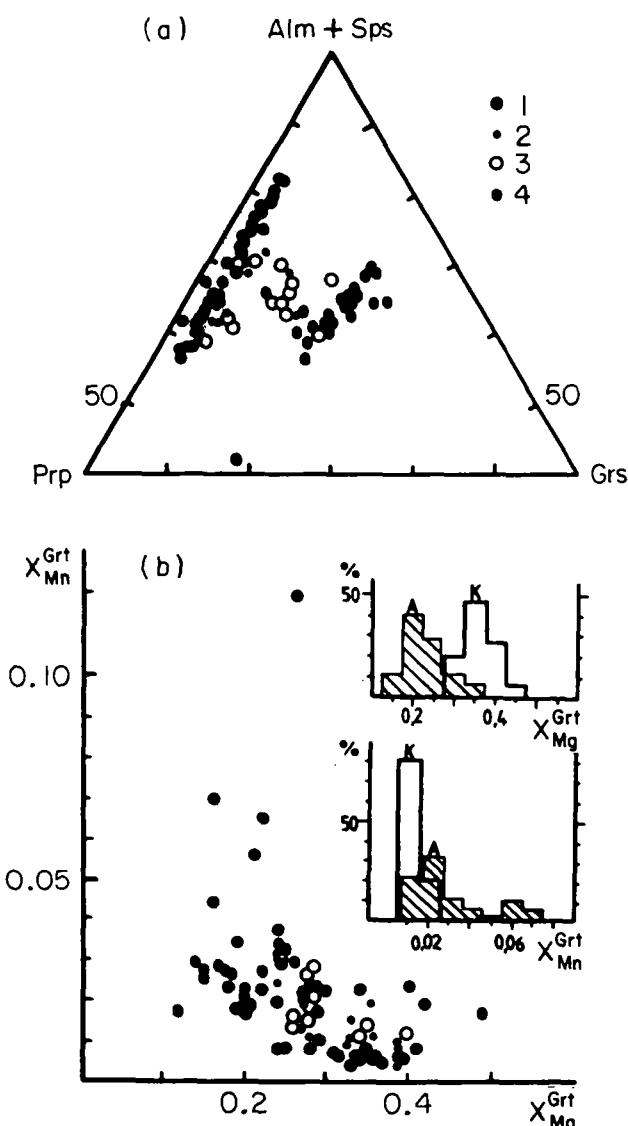


Fig. 3. Variations of garnet compositions in rocks from Atamanovskaya (A) and Kuzeevskaya (K) groups in Kanskaya formation. 1 – metapelites; 2 – garnet–biotite–hypersthene gneisses, 3 – charnockites and enderbites, 4 – metabasites.

are shown in Fig. 5 and Table 3. The table contains only those biotite analyses which were used for geothermometry.

Cordierite very rarely appears around garnets as a typical mineral of the reaction textures. In places it forms large grains growing separately in a matrix. $N_{\text{Mg}}^{\text{Crd}}$ ranges from 55 to 85 mol. % in metapelites of the Atamanovskaya group and from 68 to 86% in those from the Kuzeevskaya group (see Table 4), always increasing toward the rims of the grains. As a rule, cordierite is quite fresh and overfilled by CO₂-rich inclusions. According to the chemical analysis made by A. A. Tomilenko, the CO₂/CO₂ + H₂O (wt ratio) in cordierites varies between 0.21 and 0.65.

Spinel is a typical mineral of high-alumina gneisses. It could be seen, however, in many other rocks including metagabbroids. The most common substitutions in spinel are shown in Fig. 6. Some chemical analyses used for geothermometry and geobarometry are listed in Table 5. In places, spinel forms symplectites of magnetite and sillimanite. Intergrowth of spinel + corundum also occurs.

Orthopyroxene is mainly present in the rocks of the Kuzeevskaya group while in the Atamanovskaya group it occurs rarely. In the latter rocks $N_{\text{Mg}}^{\text{Opx}}$ ranges from 0.4 to 0.5 at Al₂O₃ content up to 5 wt %. The most aluminum-rich orthopyroxenes occur in hypersthene–sillimanite gneisses, while the most Mg-rich varieties are characteristic of metagabbroids. Diagrams in Fig. 7 reflect the $N_{\text{Mg}}^{\text{Opx}}/\text{Al}_2\text{O}_3$ ratios in orthopyroxenes from metabasites, gneisses and charnockites.

Clinopyroxene. The jadeite component in clinopyroxenes from metabasites of the Kanskaya formation is not higher than 12 mol. %, generally ranging between 3 and 7%. The ratio of Al₂O₃/Na₂O > 1.

Hornblende is a very common mineral in the Kanskaya formation rocks. Compositions are close to the edenite–pargasite solid solution. Amphiboles from metabasalts contain more TiO₂ and less Al₂O₃ than those from metagabbroids. The titanium content in hornblendes decreases with Mg number.

Feldspar in the majority of rocks from the Kanskaya formation has an approximately constant composition. Mesoperthites are similar to those described by Sandiford (1985) for granulites of the Fyfe Hills, Enderby Land, Antarctica. The anorthite content in plagioclases from the mesoperthites ranges from 40–45 mol. % and K₂O is not higher than 0.3 wt %. Plagioclase in metapelites contains about 35% anorthite component, while in metagabbro its composition varies from 50 to 80% anorthite. The albite content in alkali feldspar is not higher than 20 mol. %. Representative analyses of feldspars are listed in Table 6.

Ilmenite is a common mineral of all rock types. In metapelites and some gneisses it contains up to 1.7 wt % MgO, whereas in magmatic charnockites the MgO content is very low (nearly 0.1 wt %).

Corundum occurs exclusively in high-aluminum metapelites. Its paragenetic “satellites” are spinel, magnetite, sillimanite, cordierite and garnet. Quartz grains are separated from corundum by sillimanite rims (see Fig. 10a).

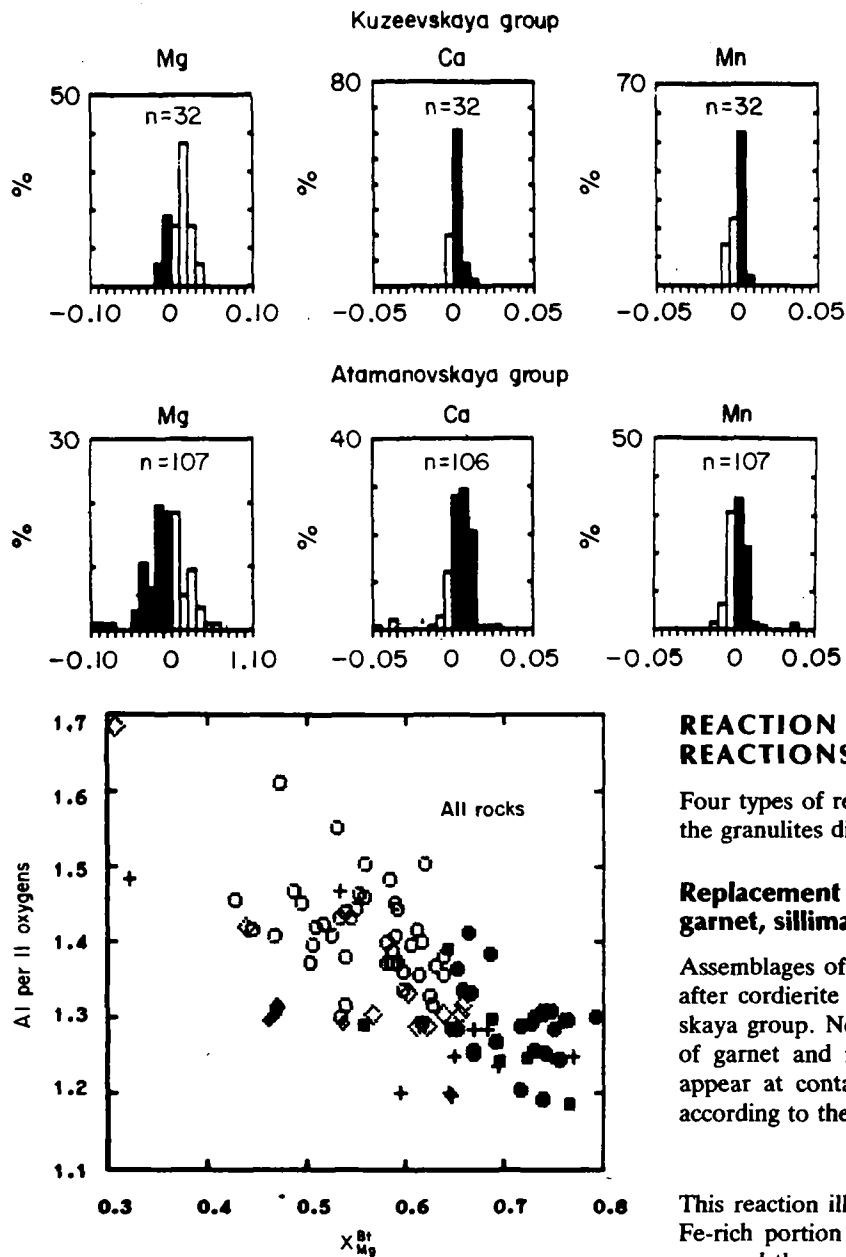


Fig. 4. Variations of Mg, Ca and Mn in garnets from metapelites of the Kanskaya formation. Histograms show differences between contents of the elements in cores (solid) and rims (open). The cores of garnets from both groups are enriched by Ca. Magnesium-rich rims are characteristic of garnets from the Kuzeevskaya group and particularly of the Atamanovskaya group.

REACTION TEXTURES AND MINERAL REACTIONS

Four types of reaction textures can be readily observed in the granulites discussed.

Replacement of cordierite by assemblages of garnet, sillimanite and quartz

Assemblages of garnet + sillimanite + quartz are formed after cordierite essentially in the rocks of the Atamanovskaya group. Newly formed skeletons or euhedral crystals of garnet and intergrowths of sillimanite + quartz may appear at contacts of garnet and cordierite (see Fig. 8) according to the reaction



This reaction illustrates schematically a breakdown of the Fe-rich portion of cordierite to produce a more Mg-rich one and the assemblage garnet + sillimanite + quartz. In sample A-258 the centres of the mineral grains involved show $N_{\text{Mg}}^{\text{Crd}} = 64$ and $N_{\text{Mg}}^{\text{Grt}} = 18$ (see Fig. 14), while at the contacts, $N_{\text{Mg}}^{\text{Crd}} = 72$ and $N_{\text{Mg}}^{\text{Grt}} = 20$. In terms of these

Fig. 5. Variations of biotite compositions from metapelites of both Atamanovskaya (●) and Kuzeevskaya (○) groups: gneisses (◊), charnockites (+), metagabbroids (D) and other metabasites (D).

Fig. 6. Isomorphic substitutions in spinel from metapelites of the Kanskaya formation. Symbols are the same as in Fig. 5.

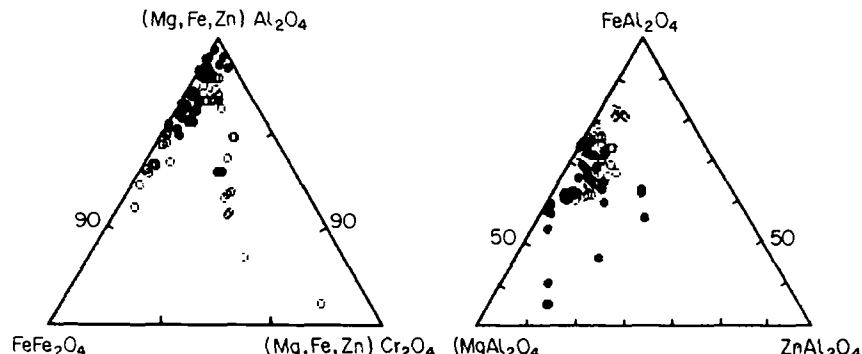
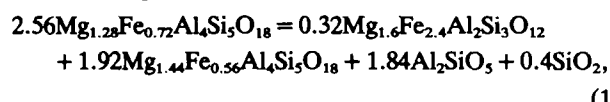


Table 5. Microprobe analysis and cation ratios in spinels from metapelites of the Atamanovskaya (A) and Kuzeevskaya (K) groups of the Kanskaya metamorphic formation.

Sample Spot no.	A-258 64	A-258 E11	A-258 E12	A-538 1	A-538 10	A-538 23	A-538 118	A-538 119	A-538 120	A-538 121	A-538 123	A-538 125	A-538 129	A-538 154	A-538 17	A-538 21
Al ₂ O ₃	56.02	56.71	56.95	56.96	52.33	49.35	55.66	55.40	57.20	58.01	56.86	58.07	58.32	54.73	52.51	51.50
Cr ₂ O ₃	0.16	0.35	0.29	1.25	3.81	5.82	2.88	2.94	0.97	0.87	1.24	1.40	1.01	3.17	3.89	4.32
FeO	34.38	34.64	34.84	29.90	37.24	37.21	30.04	30.35	28.46	28.66	27.89	27.69	28.77	30.99	37.14	38.11
MgO	5.13	5.08	4.70	5.61	3.54	2.91	6.09	5.84	6.93	6.55	7.08	7.50	6.69	6.20	3.18	3.27
ZnO	4.07	3.07	3.70	4.45	1.64	2.56	3.14	2.95	4.02	3.17	3.54	3.37	2.84	2.65	1.67	1.30
V ₂ O ₅	0.14	0.00	0.00	1.48	1.24	2.02	1.96	2.20	1.88	1.90	1.78	1.53	1.88	2.01	1.20	1.41
Total	99.90	99.85	99.85	99.65	99.80	99.87	99.77	99.68	99.46	99.16	98.39	99.56	99.51	99.75	99.79	99.91
Cations based on 4 oxygens																
Al	1.902	1.917	1.925	1.901	1.805	1.726	1.854	1.848	1.893	1.915	1.895	1.905	1.916	1.831	1.810	1.783
Cr	0.00	0.01	0.01	0.03	0.09	0.14	0.06	0.07	0.02	0.02	0.03	0.03	0.02	0.07	0.09	0.10
Fe	0.828	0.831	0.836	0.708	0.911	0.923	0.710	0.718	0.668	0.671	0.660	0.645	0.670	0.735	0.908	0.936
Mg	0.220	0.217	0.201	0.237	0.154	0.129	0.256	0.246	0.290	0.273	0.298	0.311	0.278	0.262	0.147	0.143
Zn	0.087	0.065	0.065	0.093	0.035	0.056	0.066	0.062	0.083	0.066	0.074	0.069	0.058	0.056	0.036	0.028
V	0.00	0.00	0.00	0.03	0.02	0.04	0.04	0.04	0.04	0.04	0.03	0.03	0.04	0.04	0.02	0.03
Total	3.044	3.038	3.035	2.995	3.017	3.010	2.987	2.981	2.991	2.979	2.988	2.989	2.979	2.993	3.014	3.017
X _{Mg} ^{Sp}	0.231	0.223	0.207	0.271	0.161	0.141	0.290	0.280	0.332	0.311	0.338	0.349	0.314	0.291	0.154	0.149

Sample Spot no.	A-538 24	A-538 81	A-538 84	A-643 P18	A-643 P23	A-643 P24	A-643 P66	A-643 P67	K-111 44	K-111 54	K-302 R34	K-302 R35	K-302 R38		
Al ₂ O ₃	51.05	57.01	58.32	54.79	54.90	53.83	54.20	54.52	58.59	59.23	59.09	59.31	59.04		
Cr ₂ O ₃	4.34	1.79	0.56	0.48	0.49	0.32	0.18	0.38	1.58	0.24	0.21	0.20	0.21		
FeO	37.00	28.86	30.01	38.48	38.30	39.62	39.49	38.81	28.74	29.40	32.14	31.65	31.24		
MgO	3.02	6.42	6.56	5.54	5.74	5.77	5.03	4.95	8.04	8.59	6.53	6.60	6.79		
ZnO	2.36	3.89	3.18	0.64	0.43	0.33	0.89	1.28	1.89	2.02	1.91	2.10	2.41		
V ₂ O ₅	1.83	1.60	1.19	0.00	0.00	0.00	0.00	0.00	0.80	0.46	0.00	0.00	0.59		
Total	99.60	99.57	99.82	99.93	99.86	99.87	99.79	99.94	99.64	99.94	99.88	99.89	100.28		
Cations based on 4 oxygens															
Al	1.775	1.891	1.923	1.867	1.868	1.845	1.862	1.868	1.916	1.931	1.952	1.956	1.938		
Cr	0.10	0.04	0.01	0.01	0.01	0.01	0.00	0.01	0.04	0.01	0.01	0.00	0.01		
Fe	0.913	0.679	0.702	0.930	0.925	0.964	0.963	0.943	0.667	0.680	0.753	0.740	0.728		
Mg	0.133	0.269	0.274	0.239	0.247	0.250	0.219	0.214	0.332	0.354	0.273	0.275	0.282		
Zn	0.051	0.081	0.066	0.014	0.009	0.007	0.019	0.027	0.039	0.041	0.040	0.043	0.050		
V	0.04	0.03	0.02	0.00	0.00	0.00	0.00	0.00	0.02	0.01	0.00	0.00	0.01		
Total	3.009	2.990	2.999	3.061	3.060	3.073	3.067	3.061	3.004	3.019	3.023	3.019	3.014		
X _{Mg} ^{Sp}	0.144	0.306	0.301	0.228	0.235	0.235	0.209	0.207	0.349	0.365	0.278	0.282	0.296		

mineral compositions we can write the following reaction:



i.e. cordierite ($N_{\text{Mg}}^{\text{Crd}} = 63-70$) is replaced by garnet of $N_{\text{Mg}}^{\text{Grt}} = 17-20$. Reaction (1a) corresponds to equation (1)

but might be also written in terms of the end-members of the Fe-Mg solid solutions as



The appearance of quartz and sillimanite in contact with garnet and cordierite is quite common in metapelites of the Kanskaya complex. Newly formed euhedral garnets within

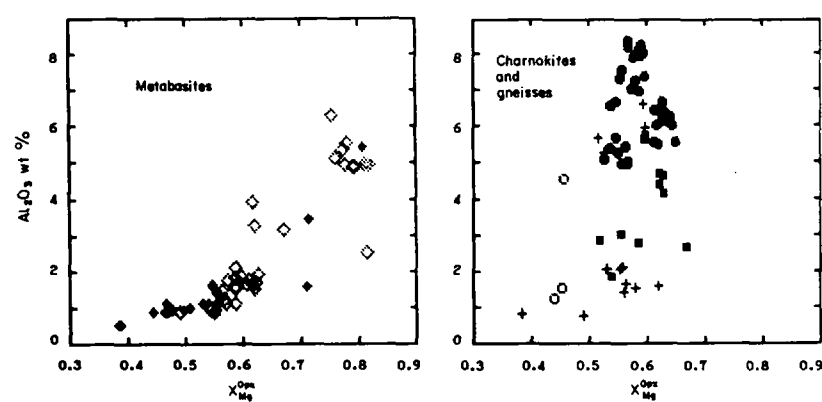


Fig. 7. Al₂O₃ versus X_{Mg}^{Op} for orthopyroxenes from rocks of the Kanskaya formation.

Table 6. Microprobe analysis and cation ratios in coexisting feldspars from metapelites of the Atamanovskaya (A) and Kuzeevskaya (K) groups of the Kanskaya metamorphic formation.

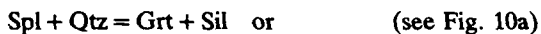
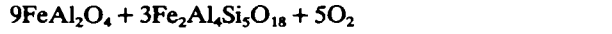
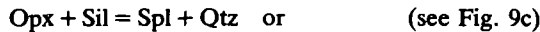
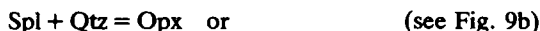
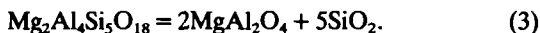
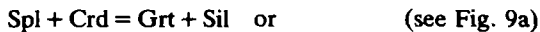
Sample Rim/core	A-269 Kfs _r	A-269 Pl _r	A-538 Kfs _r	A-538 Pl _r	A-538 Kfs _c	A-538 Pl _c	A-643 Kfs _r	A-643 Pl _r	A-643 Kfs _c	A-643 Pl _c	K-111 Kfs _r	K-111 Pl _r	K-111 Kfs _c	K-111 Pl _c	K-115 Kfs _r	K-115 Pl _r
SiO ₂	63.92	59.74	65.12	62.39	65.74	60.23	64.28	61.04	64.44	58.40	64.76	61.72	65.75	57.84	64.41	58.44
Al ₂ O ₃	17.71	24.77	18.15	23.46	17.86	25.11	17.99	24.15	17.89	24.94	17.92	23.95	18.68	26.18	18.27	25.75
CaO	0.00	7.85	0.00	5.50	0.05	6.95	0.00	6.58	0.00	8.43	0.00	6.11	0.11	8.60	0.00	8.53
Na ₂ O	0.62	7.20	1.24	8.52	2.95	7.57	1.28	8.02	1.63	7.48	1.25	7.67	3.34	6.86	1.02	7.06
K ₂ O	17.34	0.35	15.50	0.13	13.43	0.14	16.23	0.18	15.70	0.39	15.65	0.18	11.94	0.12	16.29	0.22
Total	99.59	99.91	100.01	100.00	100.00	100.00	99.78	99.97	99.66	99.64	99.58	99.63	99.82	99.60	99.99	100.00
Cations based on 8 oxygens																
Si	2.994	2.672	3.004	2.765	3.014	2.681	2.990	2.717	2.995	2.633	3.005	2.745	2.997	2.601	2.987	2.619
Al	0.978	1.306	0.987	1.226	0.965	1.317	0.986	1.267	0.980	1.325	0.980	1.255	1.004	1.388	0.999	1.360
Ca	0.000	0.376	0.000	0.261	0.002	0.331	0.000	0.314	0.000	0.407	0.000	0.291	0.005	0.414	0.000	0.410
Na	0.056	0.624	0.111	0.732	0.260	0.653	0.115	0.692	0.147	0.654	0.112	0.661	0.295	0.598	0.092	0.613
K	1.036	0.020	0.912	0.007	0.785	0.008	0.963	0.010	0.931	0.022	0.927	0.010	0.694	0.007	0.964	0.013
Total	5.064	4.998	5.014	4.991	5.026	4.990	5.054	5.000	5.053	5.041	5.024	4.962	4.995	5.008	5.042	5.015
An	0.00	36.86	0.00	26.10	0.23	33.39	0.00	30.88	0.00	37.58	0.00	30.24	0.54	40.65	0.00	39.55
Ab	5.15	61.18	10.84	73.17	24.78	65.81	10.70	68.11	13.63	60.35	10.82	68.70	29.67	58.68	8.69	59.24
Kfs	94.85	1.96	89.16	0.73	74.99	0.80	89.30	1.01	86.37	2.07	89.17	1.06	69.79	0.68	91.31	1.22

Sample Rim/core	K-115 Kfs _c	K-115 Pl _c	K-170 Kfs _r	K-170 Pl _r	K-170 Kfs _c	K-170 Pl _c
SiO ₂	64.90	58.21	63.85	59.92	64.69	58.34
Al ₂ O ₃	17.91	26.00	18.04	24.39	17.70	25.38
CaO	0.00	8.88	0.00	7.47	0.00	8.79
Na ₂ O	1.65	6.73	1.28	7.85	2.14	7.34
K ₂ O	15.54	0.18	16.62	0.25	15.15	0.15
Total	100.00	100.00	99.79	99.88	99.68	100.00
Cations based on 8 oxygens						
Si	3.002	2.608	2.797	2.682	3.002	2.619
Al	0.976	1.373	0.992	1.287	0.968	1.343
Ca	0.000	0.426	0.000	0.358	0.000	0.423
Na	0.148	0.585	0.116	0.681	0.193	0.639
K	0.917	0.010	0.989	0.014	0.897	0.009
Total	5.043	5.002	5.076	5.022	5.060	5.033
An	0.00	41.74	0.00	34.00	0.00	39.50
Ab	13.89	57.25	10.48	64.65	17.67	59.69
Kfs	86.11	1.01	89.52	1.35	82.33	0.80

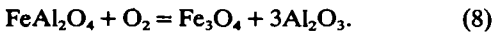
the cordierite grains (see microphoto of slide A-538 in Fig. 9a) are also characteristic of the textures.

Multiform spinel-bearing corona textures

Corona textures with spinel reflect the following net-transfer reactions involving solid solution of Spl, Opx, Crd and Grt:

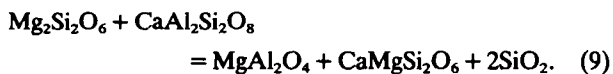
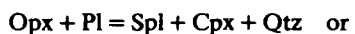


Replacement of spinel by magnetite and sillimanite according to reaction (6) may be accompanied by the following reaction



Microphotos in Fig. 9d and Fig. 10a illustrate relatively large corundum grains separated from cordierite and quartz by sillimanite rims.

In metagabbrods of the Kuzeevskaya group the spinel + quartz paragenesis appears as a result of reaction between orthopyroxene and plagioclase (see Fig. 10b)



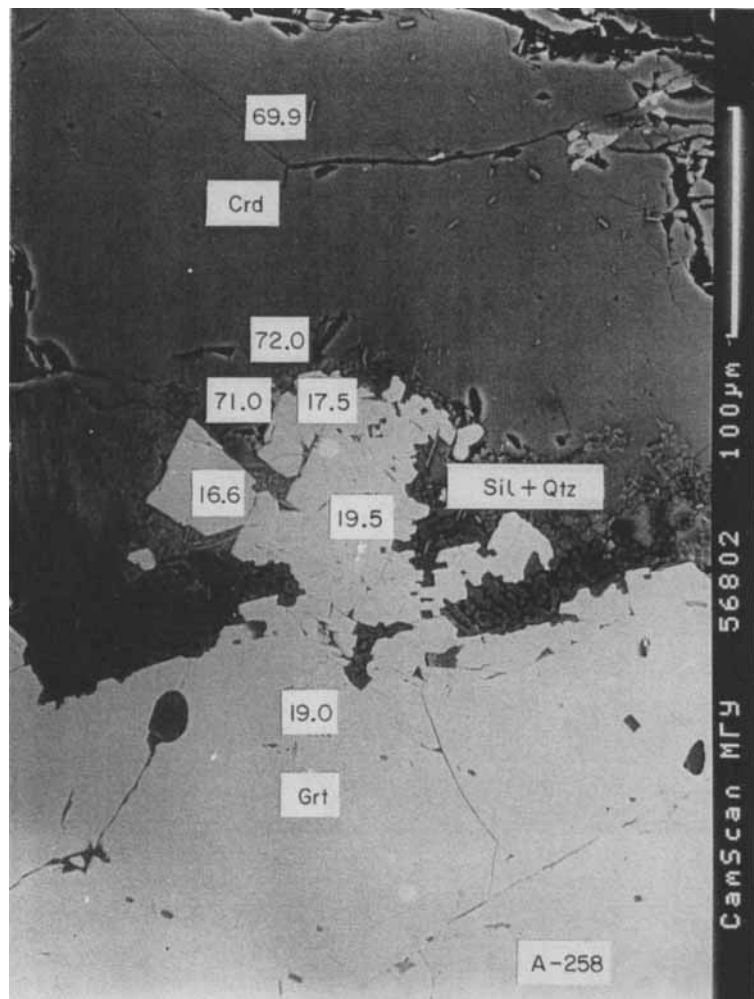
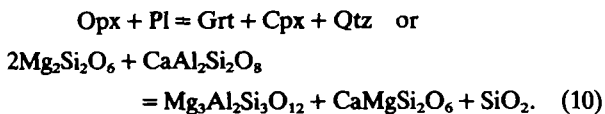


Fig. 8. Replacement of cordierite by garnet crystals and quartz–sillimanite symplectites in metapelite A-258. Reflected electrons. CamScan electronic microscope.

In metabasites reactions involving garnet are controlled by the Fe/Mg ratio in the rocks (see Fig. 2). The texture shown in Fig. 10c corresponds to the following reaction



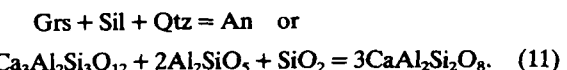
Similar textures were described by Sandiford (1985) in granulites of the Fyfe Hills, Enderby Land, Antarctica.

Reaction (10) produces garnet of relatively high and quite constant grossular content, $N_{\text{Ca}}^{\text{Gr}} = 20-25$ (see triangle in Fig. 2). The reaction reflects a decrease in temperature at relatively constant pressure (nearly “isobaric cooling” process). Garnets with $N_{\text{Ca}} = 20-25$ are widespread in the metabasites of the Kuzeevskaya group. However, the garnet rims around plagioclase can be observed just in places.

Plagioclase rims around garnet as well as the reverse

Plagioclase rims around garnet are quite common in metapelites of the Atamanovskaya as well as Kuzeevskaya

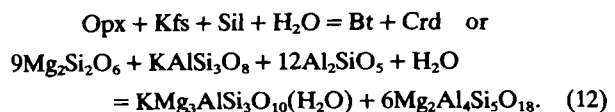
groups (See Fig. 10d). Such corona textures can be reflected by the reaction



Similar textures are common in many other granulite facies terrains. For example, such textures were described by Perchuk *et al.*, 1985) for both metapelites and metabasites of the Aldan shield.

Development of biotite and amphibole after anhydrous minerals (hydration reactions)

The hydration–dehydration reactions are widely developed in many rocks of the Kanskaya formation. In metabasites hornblende developed after pyroxenes and plagioclases, while in metapelites the secondary biotite appears via the reaction



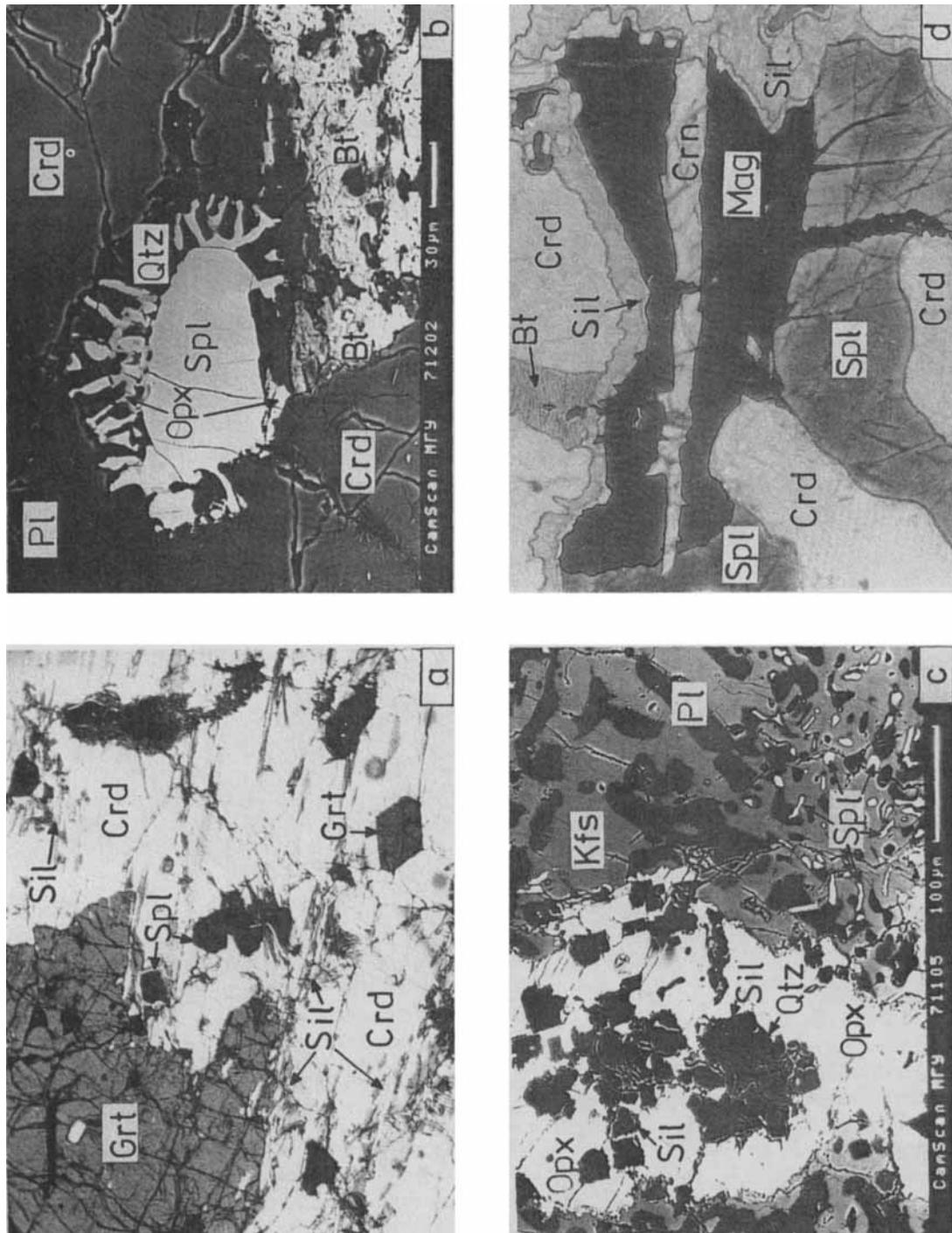


Fig. 9. Microphotos of reaction textures in granulites of the Atamanovskaya group of the Kanskaya formation. (a) Sillimanite rims around spinel (reaction 2) and growth of garnet crystals in the paragenesis of $\text{Sil} + \text{Spl} + \text{Crd}$. Sample A-538. Plane polarized light. Width of field 1.5 mm. (b) Symplectite of orthopyroxene + quartz around spinel at its contact with cordierite (reactions 3 and 4). (c) Growth of spinel and quartz instead of orthopyroxene and sillimanite in specimen K-124 (reaction 5). (d) Growth of Sil and Crn during replacement of spinel by magnetite (reactions 6 and 8). Photos (b) and (c) were taken in reflected electrons.

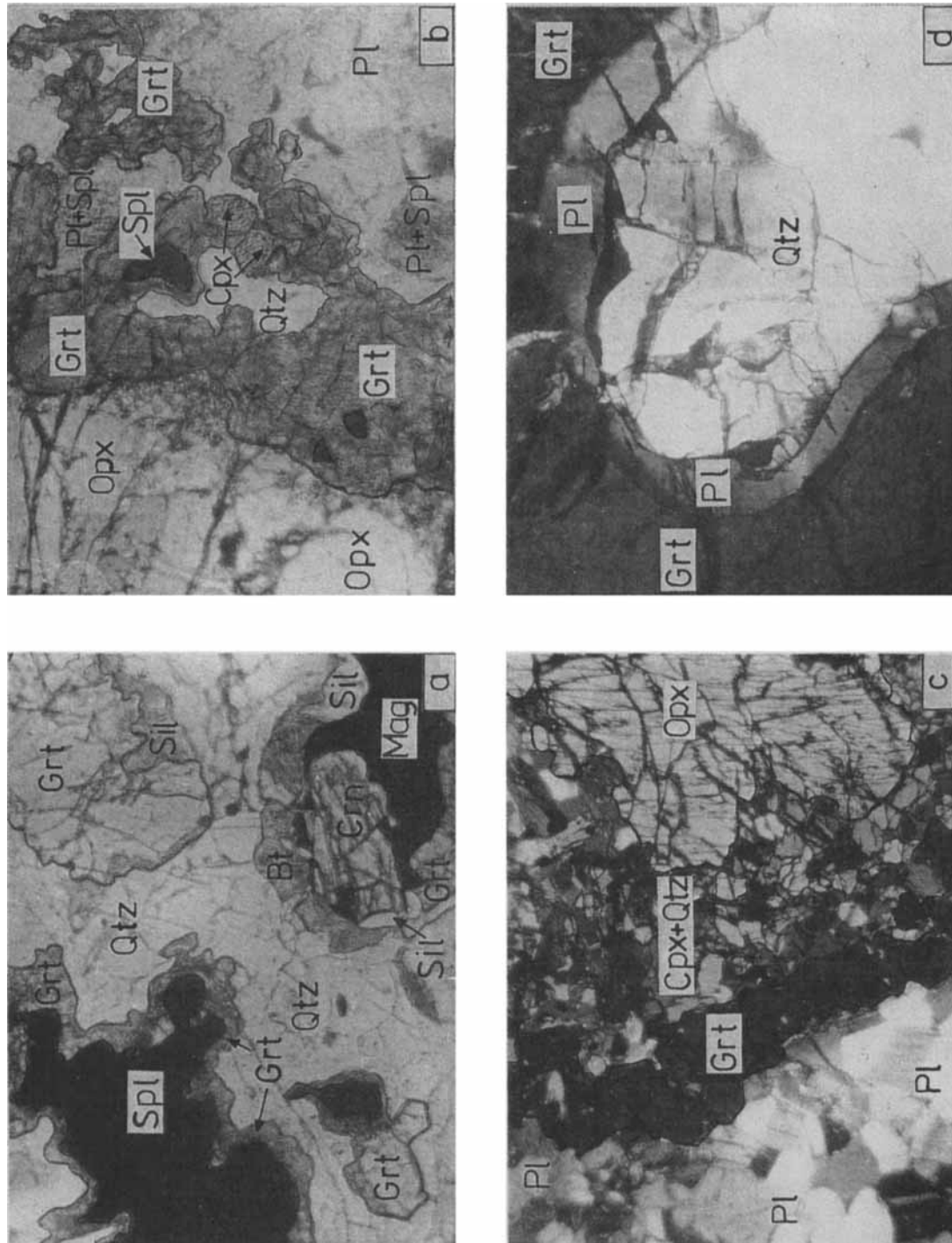


Fig. 10. Microphotos of reaction structures in metapelites and metabasites from the Kanskaya formation. (a) Rims of garnet in a contact between spinel and quartz in metapelite A-643, reaction (7). Polarized light. Width of field 2.5 mm. (b) Reactions 9 and 10 in metagabbronorite K-76: growth of garnet, spinel and quartz grains which replace orthopyroxene and plagioclase. Polarized light. Width of field 0.1 mm. (c) Quartz-clinopyroxene-garnet symplectite developed at the contact of large Opx and Pl grains in metabasite K-91, reaction (10). Nicols slightly crossed. Width of field 1.5 mm. (d) Plagioclase rim developed between garnet and quartz in metapelite K-170, reaction 11. Nicols slightly crossed. Width of field 0.05 mm.

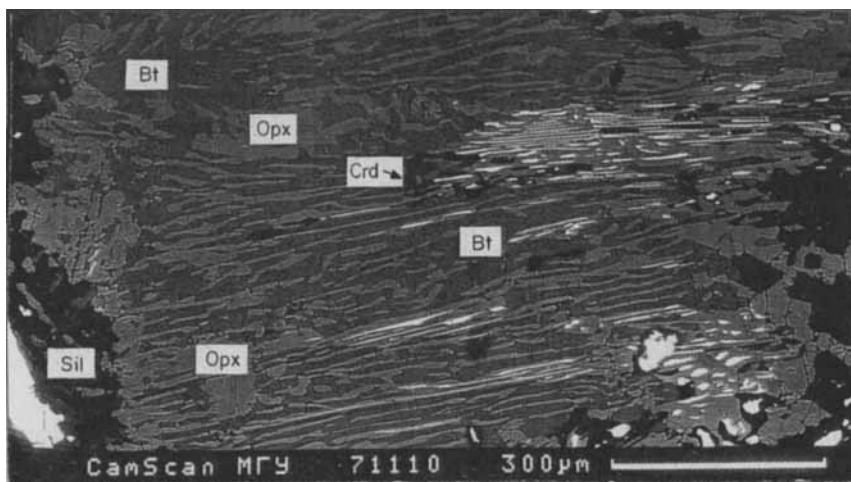
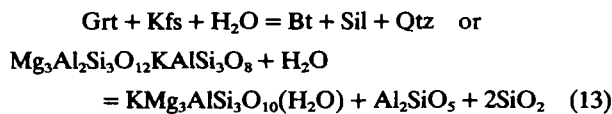


Fig. 11. Cordierite-orthopyroxene-biotite symplectite as a product of reaction (12) in metapelite K-115. Reflected electrons. CamScan electronic microscope.

In the texture of the rocks, reaction (12) is represented by the intergrowth of biotite and cordierite (see Fig. 11). Reaction (12) as well as the reaction



can be used as an indicator of the water fugacity in the course of metamorphic evolution (for example, Perchuk, 1973, 1977).

All the mineral textures discussed seem to be a result of retrogression. This suggestion is supported by data on geobarometry and fluid inclusions. In this paper we will discuss only results of the P - T estimates obtained from mineral equilibria.

GEOTHERMOBAROMETRY

After the sixties, when the first internally consistent system of geothermometers and geobarometers was created (Perchuk, 1973, 1977), several such systems for granulite facies rocks have appeared (for example, Bohlen, Wall & Boettcher, 1983; Aranovich & Podlesskii, 1983). Many of the systems are based on experimentally calibrated equilibria and used for estimating the P - T parameters in the granulite facies terranes. One of the systems created in our laboratory involves three very important equilibria: biotite-garnet and cordierite-garnet exchange reactions as geothermometers (calibration of Perchuk & Lavrent'eva, 1983) and reaction (1) as a geobarometer calibrated by Aranovich & Podlesskii (1983). A set of internally consistent geothermometers and geobarometers with spinel has been calibrated by Gerya & Perchuk (1989, see also Appendix A) on the basis of the experimentally studied equilibria mentioned and used for determinations of P - T parameters in the rocks of the Kanskaya formation (Table 8).

Using a set of geothermometric and geobarometric equations based on these experimental data Perchuk (1983, 1985, 1987, 1988) has argued the absence of

compositional evidence for prograde reactions in the granulite facies rocks. The mineral compositions (Tables 2–6) can be interpreted in terms of stages of metamorphic evolution using the Korzhinskiy local equilibrium rule.

On the basis of the above, $\text{H}_2\text{O}/\text{CO}_2$ data for cordierites and fluid inclusion studies in minerals of the rocks under consideration, N. V. Berdnikov (personal communication) has concluded that CO_2 is the main component of the metamorphic fluid. Using the cordierite-garnet geothermometer and homogenization temperatures measured by N. V. Berdnikov we have calculated the evolution paths in the diagram of Fig. 12.

The P - T diagram in Fig. 13 is drawn on the basis of geothermo-barometric data represented in Tables 7 and 8. According to fluid inclusion data, the CO_2 version of the cordierite-garnet-quartz-sillimanite geobarometer was used. An approach of "centre + centre" and "rim + rim" has been applied for estimating the P - T parameters of mineral equilibria for contacting grains of biotite, garnet,

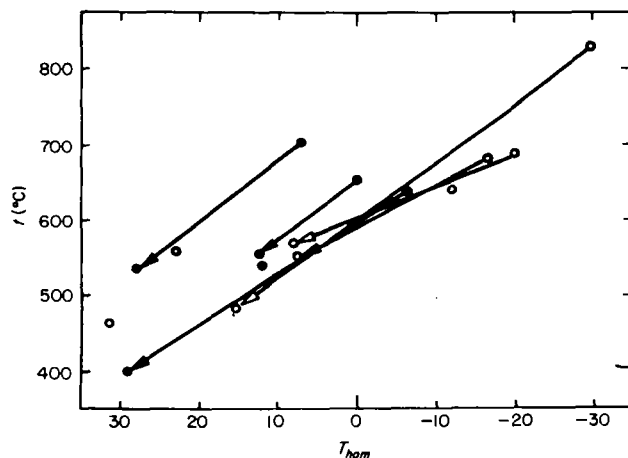


Fig. 12. Correlation of mineral equilibria temperatures with homogenization temperatures (T_{hom}) of CO_2 liquid inclusions. Both temperatures have been determined in the same specimens from the Kuzeevskaya (○) and Atamanovskaya (●) groups of the Kanskaya formation.

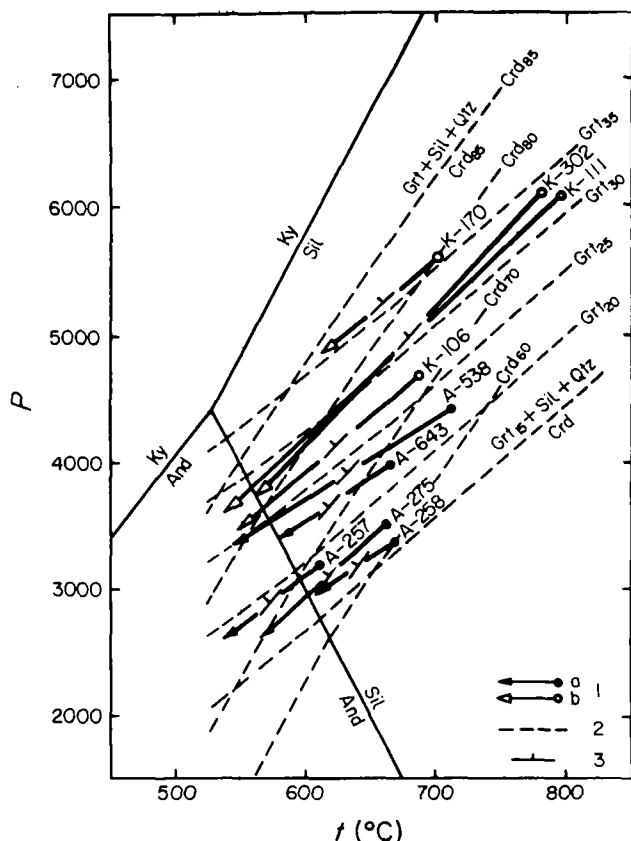


Fig. 13. P - T paths in some specimens from metapelites of the Kanskaya formation séquence. 1 – arrows show limits of P - T parameters during retrogression of the Atamanovskaya (A) and Kyseevskaya (B) sequences. 2 – isopleths of garnet and CO_2 -cordierite in the presence of sillimanite and quartz after Aranovich & Podlesskii (1983). 3 – isolines of constant amounts of minerals in reaction (1); bars show a decrease in the amount of Crd.

spinel and cordierite. The estimates correspond to limited values of the parameters in each sample chosen for geothermobarometry. Figures 12 and 13 show that the P - T paths for the rocks of the Kuzeevskaya group are located at higher pressures. This is in correlation with the widespread orthopyroxene + quartz assemblages in some metapelites of the group. In contrast, the Atamanovskaya group was formed and cooled at lower pressures. Relative location and gentle slopes of trends in Fig. 13 might reflect P - T conditions of nearly isobaric cooling for each rock collected in the different levels of an initial stratigraphic sequence. In addition, Fig. 13 shows differences in the path slopes: all paths for the Atamanovskaya group are approximately 40°C/kbar more gentle than those for the Kuzeevskaya group.

Figure 13 also shows relations between P - T paths and garnet isopleths (in coexistence with sillimanite and quartz). The slope ratios between both of these line systems explain specific features in the zoning of coexisting cordierites and garnets shown in Fig. 14. For example, in specimen A-258 garnet grows with sillimanite and quartz,

Table 7. P - T parameters of cordierite–garnet–biotite equilibria in metapelites of the Kanskaya formation.

Sample No.	Grt		Crd		Bt		t_1	P_1	t_2	dT/dP
	Spot	N_{Mg}	Spot	N_{Mg}	Spot	N_{Mg}				
A-257	42	19.3	49	68.8			609	3.2		113
	48	18.6	47	73.7			541	2.6		
	61	18.9			60	51.6			651	
	59	18.2			57	60.7			559	
A-258	1	18.2	85	63.6			665	3.4		142
	E6	19.1	E7	69.8			608	3.0		
	10	17.7			70	46.6			670	
	69	18.3			68	59.0			580	
A-269	73	19.0	71	64.7	72	51.4	654	3.6	639	62
	75	17.4	70	64.7			623	3.1		
	77	16.2			76	50.9			603	
	D17	18.2	D25	63.5			666	3.5		109
A-275	D30	18.1	D28	72.0			568	2.6		
	41	18.5			53	44.4			702	
	40	17.5			39	62.7			542	
A-538	202	22.8	26	65.5	—	—	716	4.5		141
	107	24.3	165	78.4	—	—	561	3.4		
	104	25.4			135	59.7			654	
	140	23.2			139	64.0			594	
A-643	P37	22.5	P44	68.8	P46	53.8	664	4.0	670	140
	P52	23.5	P52	76.3			580	3.4		
	P10	20.4			P14	53.3			656	
	P31	22.0			P30	61.7			600	
K-106	11	27.2	6	72.8			684	4.7		112
	5	26.0	4	80.8			550	3.5		
	9	25.6	8	77.5	16	66.0	592	3.8	590	
	2	25.2			1	70.8			553	
K-111	C5	32.1	C12	71.5			795	6.1		99
	50	27.0	49	82.4			538	3.5		
	61	35.0			60	64.6			711	
	68	32.0			67	74.6			583	
K-119	37	34.3	36	82.6			620	4.8		
	33	35.8			35	66.9			689	
	40	34.4			39	77.3			571	
	91	36.4	94	79.8			700	5.6		104
K-170	93	35.1	92	83.3	111	50.8			831	
	112	32.7			113	77.6			540	
	114	20.9								
	17	33.6	31	73.3			780	6.1		90
K-302	30	27.0	29	80.7			563	3.7		
	24	32.1			23	65.1			670	
	26	30.9			27	69.8			613	

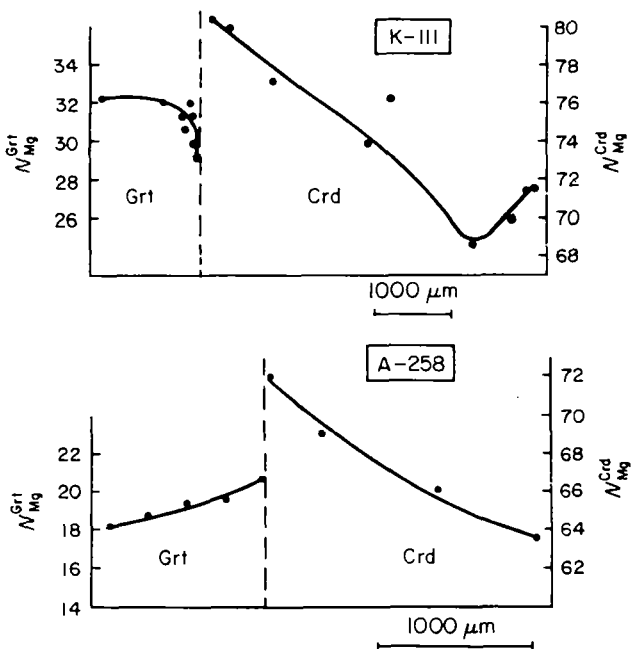
replacing cordierite with decreasing temperature. Sketch A-258 in Fig. 14 shows an increase in Mg number in both cordierite and garnet. Just at the junction of these grains $N_{\text{Mg}}^{\text{Grt}}$ slightly decreases reflecting the Fe–Mg diffusion exchange. The P - T path for this sample slightly intersects the garnet isopleths in Fig. 13.

In the case of sample K-111 the P - T path in Fig. 13 does not intersect the garnet isopleth and, as a result, a change in N_{Mg} of the attached cordierite and garnet shows the reverse profiles (see Fig. 14, sketch K-111).

The P - T estimates are restricted by the data of Tables 7 and 8. As mentioned above, these tables show the results of the “centre + centre” and “rim + rim” approach used

Table 8. $P-T$ parameters of spinel-bearing paragenesis in metapelites of the Kanskaya formation.

Sample No.	Grt			Crd			Spl			P_1	P_2
	Spot	N_{Mg}	N_{Ca}	Spot	N_{Mg}	Spot	N_{Mg}	N_{Cr}	t (°C)	(kbar)	
$Grt_{Mg} - 2Sil = Crd_{Mg} + Spl_{Mg}$											
A-538	3	24	2.0	2	75	1	26	1.5	603	3.6	3.7
	148	28	2.7	149	79	119	26	3.4	603	4.1	4.1
	126	25	2.4	127	79	123	32	1.4	555	3.3	3.4
	124	25	2.0	127	79	125	34	1.6	559	3.4	3.5
	130	28	2.3	128	80	129	30	1.2	572	3.8	3.7
	105	26	3.3	162	77	121	30	1.0	607	3.8	3.9
	105	26	3.3	164	76	84	29	0.7	620	3.9	4.0
	105	26	3.3	162	77	120	32	1.1	607	3.7	3.9
	103	24	2.9	151	75	118	28	3.3	608	3.5	3.7
	153	26	1.7	152	77	154	28	3.7	596	3.7	3.8
	100	27	2.4	155	79	81	29	2.1	581	3.8	3.8
A-258	66	25	1.1	65	72	64	23	0.2	660	4.2	4.3
	E8	20	1.3	E9	71	E11	22	0.4	590	3.1	3.1
	E8	20	1.3	E14	74	E11	22	0.4	551	3.0	2.8
	E8	20	1.3	E13	72	E12	21	0.4	575	3.1	3.0
K-111	42	27	3.2	50	82	44	34	1.8	544	3.6	3.6
K-302	33	31	2.4	36	83	34	28	0.3	575	4.4	4.1
	33	31	2.4	37	80	35	28	0.2	626	4.6	4.5
	32	33	3.2	40	76	39	29	0.3	708	5.1	5.4
	43	32	3.4	39	78	38	29	0.3	662	4.8	4.9
$1/3Grt_{Mg} + 2/Sil = 5/3Qtz + Spl_{Mg}$											
K-111	53	29	3.3	—	—	54	36	0.3	568	—	4.1
	56	30	3.2	—	—	54	36	0.3	576	—	4.1
A-643	P64	19	2.9	—	—	P67	21	0.5	587	—	3.2
	P65	17	3.1	—	—	P66	21	0.2	538	—	3.3
	P17	21	2.4	—	—	P18	23	0.6	595	—	3.3
	P25	20	2.9	—	—	P24	23	0.4	577	—	3.4
	P26	21	3.4	—	—	P23	23	0.6	583	—	3.3
$Spl_{Mg} + 5/2Qtz = 1/2Crd_{Mg}$											
A-538	—	—	—	18	66	10	16	4.5	662	—	3.6
	—	—	—	13	66	17	15	4.6	645	—	3.2
	—	—	—	22	66	21	14	5.6	643	—	3.0
	—	—	—	25	64	23	13	7.0	663	—	3.3
	—	—	—	25	64	24	14	5.2	655	—	3.2

**Fig. 14.** Common chemical zoning in garnets in contact with cordierite in samples from the Kuzeevskaya and Atamanovskaya groups.

for calibration of $P-T$ parameters. According to Fig. 14, several $P-T$ estimates have been done on the basis of data on intermediate compositions of minerals presumably equilibrated. These data are in good agreement with the $P-T$ paths in Fig. 13.

A MODEL FOR EVOLUTION OF REGIONAL METAMORPHISM

A peak of metamorphism is recorded by the orthopyroxene + quartz + sillimanite paragenesis met in the Kuzeevskaya sequence group. Unfortunately, there are no robust geothermometers and geobarometers to measure $P-T$ parameters of the rocks. However, in comparing the paragenesis with that from the Aldan shield formations (Perchuk *et al.*, 1985) and the Fyfe Hills complex, Enderby Land, Antarctica (Sandiford, 1985) we can propose the following peak metamorphic conditions: $t \geq 900^\circ\text{C}$ and $P \geq 8$ kbar. Thus, a drop in temperature and pressure from these values to 790°C and 6 kbar reflects the first stage of metamorphic evolution of the Kanskaya formation, supposedly in the Late Archaean.

The results shown in Fig. 13 are the basis for creation of a model for the second stage of metamorphic evolution of the Kanskaya formation. In addition, we have to take into account the following observations:

1. Stratigraphy of the Precambrian in the Yenisey range (Gerya *et al.*, 1986, page 12) is in good agreement with geothermometric data, i.e.

(a) The thickness of the Kuzeevskaya group is about 3000 m. It corresponds approximately to the difference in pressure estimates for the samples taken from upper and lower levels of the Kuzeevskaya sequence group (see Table 5 and Fig. 13).

(b) The thickness of the Atamanovskaya group is about 2500–3000 m and corresponds to the pressure difference of around 1 kbar estimated from mineral geobarometry (see Table 5 and Fig. 13).

(c) The total thickness of the Kanskaya formation found from geological mapping corresponds to the vertical pressure gradient ≈ 2.2 kbar.

2. The peaks of $P-T$ parameters estimated from the "centre + centre" composition ratios of the touching cordierite and garnet can reflect the Archaean geotherm (in this area) of nearly 45°C/kbar .

3. The samples collected from different levels of the stratigraphic sequence have recorded information on the regimes of uplift and cooling of the Kanskaya formation.

4. The hypersthene–sillimanite–quartz assemblages in the cross section through the Kanskaya formation toward the Tarakskiy pluton are replaced by cordierite–garnet in metapelites. This is in agreement with steeper slopes ($\approx 100^\circ\text{C/kbar}$) of $P-T$ paths and with faster uplift of the rocks involved in the granite–gneiss dome structure.

5. The shallower slope ($\approx 140^\circ\text{C/kbar}$) of $P-T$ paths from areas farthest from the Tarakskiy pluton occurs in granulite facies rocks in which replacement of cordierite by garnet + sillimanite + quartz is observed.

6. Replacement of plagioclase by garnet in metagabrods of the Kuzeevskaya group.

These features of the Kanskaya formation contrast with the majority of the Precambrian granulite facies terranes studied before. Sandiford (1985) reported similar reaction textures in granulites of the Fyfe Hills complex, Enderby Land, Antarctica and suggested a sub-isobaric P - T path, which differs from the paths shown in Fig. 13. Harley (1988) observed the P - T evolution for over 90 terranes and discussed the origin of sub-isobaric and sub-isothermic retrogressions. However, he did not mention retrogressions for different portions of the same complex as described above for the Kanskaya formation; high dT/dP trajectories in Fig. 13 are the most exciting feature of the formation.

In the majority of cordierites from Precambrian metapelites only short-distance diffusion zoning occurs. There are no experimental data on Fe-Mg diffusion coefficients for cordierites. However, according to Lasaga (1983), these coefficients might be several orders of magnitude smaller than for garnet and, as a result, high temperature ($t \geq 700^\circ\text{C}$) chemical zoning may be preserved in cordierites if the cooling rate is relatively high. The Kanskaya formation is presumably an example of such a cooling history in the Late Proterozoic, when Tarakskiy granite pluton was formed.

Comparison of the results obtained with data on other P - T paths among granulite facies complexes in eastern Siberia (Perchuk, 1989; Perchuk *et al.*, 1985) shows that the thermal history of the Kanskaya formation is unique. There is only one way to estimate details of the history of excavation of Archaean gneisses from the base of the crust (e.g. O'Hara, 1977), i.e. by studying the metamorphic reactions in detail. The granulites studied provide a good example of this method. In connecting high-grade ends of the paths in the diagram of Fig. 13 we can locate the Archaean geotherm beneath the Kanskay block as shown in Fig. 15. Arrows in this diagram indicate nearly isobaric cooling of each layer of the sequence in the Proterozoic. By this, slopes of the arrows reflect very slow uplift of the Kanskaya formation with respect to the cooling rate.

The model proposed is supported by mineral reactions in the metaigneous rocks of the Kanskaya formation. The ultramafic-mafic magma intruded into rocks under granulite facies P - T conditions during Archaean time. According to the bulk composition of the olivine-bearing metagabbro (Gerya *et al.*, 1986), the liquidus temperature calculated after Perchuk's formula (1987) at 6 kbar pressure is about 1350°C . Nearly isobaric cooling of the formation up to the Archaean geotherm from 1350° to $\approx 750^\circ\text{C}$ led to the eclogitization process, particularly in the iron-rich rocks. The late metamorphic evolution of the rocks was entirely associated with the course of metamorphism of the Kanskaya sequence.

Formation of the Tarakskiy granite pluton affected the metamorphic evolution of the Kanskaya formation. Growth of the granite-gneiss dome led to acceleration of uplift of the formation in the Middle Proterozoic. This change in the speed of ascent has been precisely recorded by mineral reactions in the Atamanovskaya group rocks. These show steep gradients ($dT/dP \approx 10^\circ\text{C/kbar}$).

Korzhinskiy (1936, 1945) suggested that regional

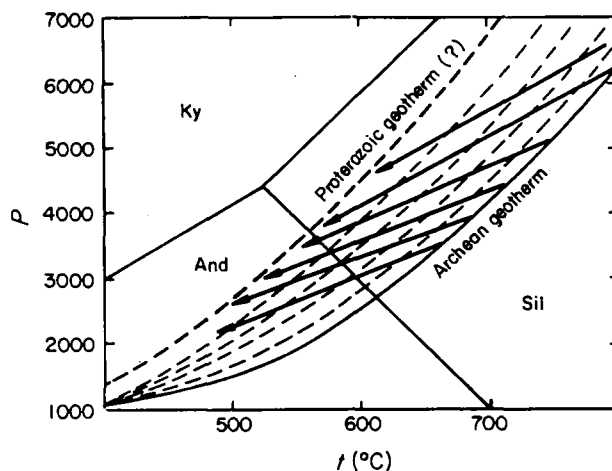


Fig. 15. The course of metamorphism in the Kanskaya formation as a result of gradual change of P and T from the Archaean geotherm to the Proterozoic (?) one through intermediate states (dashed lines). Arrows trace near isobaric cooling of separate layers of different portions in the Kanskaya formation.

Isotopically dated Archaean geotherm was deduced by connecting the high P - T limits for all samples in Fig. 13. These data indicate relatively fast cooling of the Archaean sequence during the Proterozoic when Tarakskiy pluton was formed.

metamorphism in the Precambrian beneath the marginal portion of the Siberian platform is caused by the deep-seated magmatic activity. He (Korzhinskiy, 1968) further suggested a model for generating the energy for metamorphic reactions from the mantle fluid-magmatic sources. This general statement was greatly advanced by Wells (1980, 1981), England & Richardson (1977), England & Bickle (1977) who created semi-quantitative thermal and dynamic models for regional metamorphism in direct relation with magmatic activity. Intrusion of mafic and ultramafic magmas during granulite facies metamorphism is a sign of mantle magmatism beneath the thick continental crust in the marginal portion of the Siberian platform. In order to make a greater effort and relate more quantitatively the described petrographic details with magmatic activity, the fluid regime of metamorphism of the Kanskaya granulite facies rocks must be discussed. This topic will be a fruitful area for future studies.

ACKNOWLEDGEMENTS

All microprobe analyses of minerals were made with a CamScan + Link H.E.D.A. system in the laboratory of electron microscopy and microanalysis at the Department of Petrology, Moscow State University. We thank L. B. Granovskiy, N. G. Zinov'eva, N. A. Karataeva and M. A. Korovkin for assistance while working with the microprobe. We also thank Steve Bohlen and Dex Perkins for their helpful reviews and productive discussions. We are grateful for discussion of the work with Mike Brown, Alan Thompson, Kalevi Korsman, Thom Frish and Bas Hensen during the 'Granulite' conference in Clermont Ferrand (September, 1988).

APPENDIX A

A set of internally consistent geothermometers and geobarometers involving spinel (see Table A1) was calibrated on the basis of experimentally studied biotite-garnet and cordierite-garnet exchange equilibria (Perchuk & Lavrent'eva, 1983) and the garnet-cordierite-sillimanite-quartz net-transfer reaction (Aranovich & Podlesskii, 1983). Temperatures for spinel(Spl)-garnet(Grt) and cordierite(Crd)-spinel geothermometers can be calculated after the following formula:

$$T = \frac{\Delta H^\circ + \Delta V^\circ P + H_{Mg}^e - H_{Fe}^e - H_{Cr-Fe}^e + H_{Cr-Mg}^e + H_{Ca}^e(\text{Grt})}{R \ln K_D^{(1,2)} + \Delta S^\circ + S_{Mg}^e - S_{Fe}^e - S_{Cr-Fe}^e + S_{Cr-Mg}^e + S_{Ca}^e(\text{Grt})} \quad (\text{A1})$$

where $R = 1.987 \text{ cal/K}$ and standard values for reactions A2 and A3 are listed in Table A1

$$K_D^{(1)} = \left(\frac{X_{Mg}}{1 - X_{Mg}} \right)^{\text{Grt}} * \left(\frac{1 - X_{Mg}}{X_{Mg}} \right)^{\text{Spl}} \quad (\text{A2})$$

$$K_D^{(2)} = \left(\frac{X_{Mg}}{1 - X_{Mg}} \right)^{\text{Spl}} * \left(\frac{1 - X_{Mg}}{X_{Mg}} \right)^{\text{Crd}} \quad (\text{A3})$$

Other terms in equation (A1) can be calculated with the following equations:

$$\begin{aligned} H_{Mg}^e &= [(2W_{Mg}^H - W_{Fe}^H) - 2(W_{Fe}^H - W_{Mg}^H)X_{Fe}^{\text{Spl}}] * (X_{Fe}^{\text{Spl}})^2, \\ H_{Fe}^e &= [(2W_{Fe}^H - W_{Mg}^H) + 2(W_{Fe}^H - W_{Mg}^H)X_{Mg}^{\text{Spl}}] * (X_{Mg}^{\text{Spl}})^2, \end{aligned} \quad (\text{A7})$$

No. (r)	Reaction	ΔH_{1000}° (cal)	ΔS_{1000}° (cal/K)	ΔV° (cal/bar)
A2	Grt _{Mg} + Spl _{Fe} = Grt _{Fe} + Spl _{Mg}	-3902	-3.535	-0.0089
A3	Crd _{Fe} + Spl _{Mg} = Crd _{Mg} + Spl _{Fe}	-2232	0.867	-0.0265
A4	Grt _{Mg} + 2Sil = Crd _{Mg} + Spl _{Mg}	-3403	6.851	1.4387
A5	$\frac{1}{3}\text{Grt}_{Mg} + \frac{2}{3}\text{Sil} = \frac{2}{3}\text{Qtz} + \text{Spl}_{Mg}$	-3415	-2.345	0.1622
A6	$\frac{1}{2}\text{Spl}_{Mg} + \frac{1}{2}\text{Qtz} = \frac{1}{2}\text{Crd}_{Mg}$	3421	6.943	0.4760

REFERENCES

- Aranovich, L. Ya. & Podlesskii, K. K., 1983. The cordierite-garnet-sillimanite-quartz equilibrium: experiments and applications. *Advances in Physical Geochemistry*, 3, 173-198.
- Artemov, Yu. M., 1963. Geochronology of some rocks from southern portion of the Tarakskiy pluton in the Yenisey range. *Geokhimiia*, 2, 174-178.
- Bohlen, S. R., Wall, V. J. & Boettcher, A. L., 1983. Geobarometry in granulites. *Advances in Physical Chemistry*, 3, 141-171.
- England, P. C. & Bickle, P., 1984. Continental thermal and tectonic regimes during the Archean. *Journal of Geology*, 92, 353-367.
- England, P. C. & Richardson, S. W., 1977. The influence of erosion upon the mineral facies of rocks from different metamorphic environments. *Journal of the Geological Society, London*, 134, 201-213.
- Gerling, E. K. & Artemov, Yu. M., 1964. Absolute Geochronology of southern and central part of the Yenisey range. *Geokhimiia*, 7, 610-622.
- Gerya, T. V., Dotsenko, V. M. & Zabolotskiy, K. A., 1986. *Precambrian crystalline complexes of the Enisey Mountain-Ridge: Guide-Book*, Nauka Press, Novosibirsk (in Russian).
- Gerya, T. V. & Perchuk, L. L., 1989. Spinel bearing geothermometers and geothermometers. *Geokhimiia* in press.
- Harley, S., 1988. Granulite $P-T$ paths: constraints and implications for granulite genesis. *Terra cognita*, 8, 267-268.

$$\begin{aligned} S_{Mg}^\circ &= [(2W_{Mg}^S - W_{Fe}^S) - 2(W_{Fe}^S - W_{Mg}^S)X_{Fe}^{\text{Spl}}] * (X_{Fe}^{\text{Spl}})^2, \\ S_{Fe}^\circ &= [(2W_{Fe}^S - W_{Mg}^S) + 2(W_{Fe}^S - W_{Mg}^S)X_{Mg}^{\text{Spl}}] * (X_{Mg}^{\text{Spl}})^2, \end{aligned} \quad (\text{A8})$$

where $W_{Mg}^H = -351$; $W_{Mg}^S = -1.013$; $W_{Fe}^H = -1046$; $W_{Fe}^S = -1.395$; $H_{Ca}^{\text{Grt}} = 995 * X_{Ca}^{\text{Grt}}$; $S_{Ca}^{\text{Grt}} = 3.720 * X_{Ca}^{\text{Grt}}$; $H_{Cr-Mg}^{\text{Spl}} = 2875 * (X_{Fe}^{\text{Spl}})^2 * X_{Cr}^{\text{Spl}}$; $S_{Cr-Mg}^{\text{Spl}} = -1.445 * (X_{Fe}^{\text{Spl}})^2 * X_{Cr}^{\text{Spl}}$; $H_{Cr-Fe}^{\text{Spl}} = -8298 * (X_{Mg}^{\text{Spl}})^2 * X_{Cr}^{\text{Spl}}$; $S_{Cr-Fe}^{\text{Spl}} = -0.139 * (X_{Mg}^{\text{Spl}})^2 * X_{Cr}^{\text{Spl}}$; $X_{Ca}^{\text{Grt}} = \text{Ca}/(\text{Ca} + \text{Fe} + \text{Mn} + \text{Mg})$; $X_{Fe}^{\text{Spl}} = \text{Fe}/\text{Mg} + \text{Fe}$; $X_{Mg}^{\text{Spl}} = \text{Mg}/\text{Mg} + \text{Fe}$ and $X_{Cr}^{\text{Spl}} = \text{Cr}/(0/2)$.

Geobarometric equations related to reactions (A4)-(A6) in Table A1 can be derived from the following fundamental formula:

$$P = \frac{\Delta H_{(r)}^\circ + \Delta S_{(r)}^\circ * T + RT \ln K_{(r)} + G_{Mg}^\circ + G_{Cr-Mg}^\circ + \Phi_G^\circ}{\Delta V_{(r)}^\circ + \Delta V_{(r)}^e + \Phi_V^\circ}, \quad (\text{A9})$$

where $\Delta V_{(r)}^\circ \approx 0$; $K_{(A4)} = (X_{Mg}^{\text{Crd}})^2 * X_{Mg}^{\text{Spl}} / (X_{Mg}^{\text{Grt}})^3$; $K_{(A5)} = X_{Mg}^{\text{Spl}} / X_{Mg}^{\text{Grt}}$; $K_{(A6)} = X_{Mg}^{\text{Crd}} / X_{Mg}^{\text{Spl}}$. Φ -functions depend on the number of Crd moles n in reaction r and are as follows:

System	Φ_G°	Φ_V°
Crd (dry)	0	0
Crd-CO	$(18 + 0.8286 * T) * n$	$-0.37228 * n$
Crd-H ₂ O	$(-2414 + 1.9552 * T) * n$	$-0.37228 * n$

Table A1. Geothermobarometric reactions involving spinel and their standard thermodynamic values.

- Datsenko, V. M., 1984. *Granitoid magmatism of S. W. foldbelt framing the Siberian Platform*. Nauka Press, Moscow (in Russian).
- Korzhinskiy, D. S., 1936. Analyses of mineral paragenesis in the Archean crystalline schists of southern Baikal Lake shore. *Zapiski Vserossiyskogo Mineralogicheskogo Obshestva*, 65(2), (in Russian).
- Korzhinskiy, D. S., 1945. A regularity in mineral assemblages of the Archean rocks of eastern Siberia. *Trudy Instituta Geologicheskikh Nauk SSSR*, 61 (in Russian).
- Korzhinskiy, D. S., 1968. Transmagmatic fluids of the mantle origin and their role in magmatism and metamorphism. In: *The Crust and Upper Mantle*, pp. 26-41. Nauka Press, Moscow (in Russian).
- Kuznetsov, Yu. A., 1941. *Petrology of the Yenisey Range. Data on geology of Western Siberia*, 15 (57), Tomsk (in Russian).
- Lasaga, A. C., 1983. Geospeedometry: An extension of geothermobarometry. *Advances in Physical Chemistry*, 3, 81-115.
- Lavrent'eva, I. V., 1983. On the regression in metamorphic rocks of the Hankay massif, Far East. *Mineralogical Journal*, 3, 65-76, (in Russian).
- Nozhkin, A. D., 1983. Early Precambrian gneiss complexes of the Yenisey range and their geochemical peculiarities. *Geologia and Geofizika*, 9, 3-11.
- Nozhkin, A. D., Malishev, V. I. & Sumin, A. V., 1989. The age of the metamorphic complexes of S. W. portion of the Siberian Platform from the U-Pb studies. *Geologia and Geofizika*, in press.

- O'Hara, M. J., 1977. Thermal history of excavation of the Archean gneisses from the base of the crust. *Journal of the Geological Society, London*, **134**, 185–200.
- Perchuk, L. L., 1973. *Thermodynamical regime of deep-seated petrogenesis*. Nauka Press, Moscow (in Russian).
- Perchuk, L. L., 1977. Thermodynamical control of metamorphic processes. In: *Energetics of Geological Processes*, (eds Saxena, S. K. & Bhattacharji, S.), pp. 285–352, Springer-Verlag, New York.
- Perchuk, L. L., 1983. Thermodynamic aspect of polymetamorphism. In: *Metamorphic zonation and polymetamorphic complexes* (eds Dobretsov, N. L. & Budanov, V. I.), pp. 134–140, Nauka Press, Moscow (in Russian).
- Perchuk, L. L., 1985. Metamorphic evolution of shields and foldbelts. *Geologicky Zbornik-Geogica Carpatica*, **36**, Bratislava, 179–189.
- Perchuk, L. L., 1987. The course of metamorphism. *International Geology Review*, **28**, 1377–1400.
- Perchuk, L. L., 1989. *P-T*-fluid regimes of metamorphism and related magmatism with specific reference to the Baikal granulites. In: *Evolution of Metamorphic Belts*, (eds Daly, S. Yardley, B. W. & Cliff, R.). Geological Society of London, Special Publication, in press.
- Perchuk, L. L., Aranovich, L. Ya., Podlesskii, K. K., Lavrent'eva, I. V., Gerasinov, B. Yu., Fed'kin, V. V., Kitsal, V. I., Karsakov, L. P. & Berdnikov, N. V., 1985. Precambrian granulites of the Aldan shield, eastern Siberia, USSR. *Journal of Metamorphic Geology*, **3**, 265–310.
- Perchuk, L. L., Kitsul, V. I., Podlesskii, K. K., Gerasimov, V. Yu., Aranovich, L. Ya. & Fed'kin, V. V., 1981. *Metamorphic evolution of the Aldan Massif*. Yakutian Branch of the USSR Academy of Sciences, Yakutian Press, 63 pp. (in Russian).
- Perchuk, L. L. & Lavrent'eva, I. V., 1983. experimental investigation of exchange equilibria in the system cordierite–garnet–biotite. In: *Advances in Physical Chemistry*, **3**, pp. 199–299, Springer-Verlag, New York.
- Phillips, G. N., Wall, V. J., 1981. Evaluation of prograde regional metamorphic conditions: their implications for heat source and water activity during metamorphism in the Willyam Complex, Broken Hill, Australia. *Bulletin of Mineralogy*, **104**, 801–810.
- Sandiford, M., 1985. The metamorphic evolution of granulites at Fyfe Hills: implications for Archean crustal thickness in Enderby Land, Antarctica. *Journal of Metamorphic Geology*, **22**, 155–179.
- Serenko, V. P., 1969. New data on metamorphism of the southern part of the Yenisey range. *Geologia and Geophysika*, **9**, 136–141.
- Volobuev, M. I., Zykov, S. I. & Stupnikova, N. I., 1980. Geochronology of Precambrian granitoids of the Eastern Sayan and Western Pribaikal'e. In: *Geochronology of Eastern Siberia and Far East*, pp. 66–79, Nauka Press, Moscow (in Russian).
- Waters, D. J., 1988. Metamorphic processes, tectonics, and the record of prograde *P-T* evolution in granulites. *Terra cognita*, **8**, 268–269.
- Wells, P. R. A., 1980. Thermal models for the magmatic accretion and subsequent metamorphism of continental crust. *Earth and Planetary Science Letters*, **46**, 253–265.
- Wells, P. R. A., 1981. Accretion of the continental crust: thermal and geochemical consequences. *Philosophical transactions of the Royal Society London*, **A**, **301**, 347–357.

Received 5 September 1988; revision accepted 28 February 1989.